CODEN:LUTEDX/(TEIE-5506)/1-40/(2024)

Industrial Electrical Engineering and Automation

Local Voltage Control in Converter Based PV Generation

Feasibility of an Active Control Method in Low Voltage Distribution Networks

Charlotta Sporre

Division of Industrial Electrical Engineering and Automation
Faculty of Engineering, Lund University

Lunds Tekniska Högskola

Master Thesis

Division of Industrial Electrical Engineering and Automation

Local Voltage Control in Converter Based PV Generation

Feasibility of an Active Control Method in Low Voltage Distribution Networks

Author
Charlotta Sporre
ch4265sp-s@student.lu.se

January 2024

Supervisor
Olof Samuelsson, olof.samuelsson@iea.lth.se
Examiner
Jörgen Svensson, jorgen.svensson@iea.lth.se
Assistant Supervisor
Martin Lundberg, martin.lundberg@iea.lth.se

Abstract

As the world is trying to rid itself of its dependence on fossil fuels, the need for renewable energy is rapidly increasing. In the power distribution network (DN), this takes the form of distributed generation (DG) from renewable sources, such as photovoltaic (PV) power production. But as more DG is installed, it can lead to issues in the DN such as overloading and overvoltage when production is high. Today, in order to combat these issues, the DN is reinforced, which might be costly, and take time.

This thesis has instead studied an alternative to network reinforcement, active network management (ANM), in order to avoid overvoltage. By implementing PI controllers in converter based DG, the power output from the DG can be curtailed, and thus reducing the voltage locally. By implementing local control of the power output in the DG, the voltage is kept within allowed limits across the feeder.

In this thesis, one such ANM method was studied, which implements delta control of the active power produced by PV, in order to avoid overvoltage in a low voltage (LV) DN. Stability of the method has previously been shown analytically. In this thesis, the method was studied numerically in order to analyse the performance of the controllers in different test systems. The test systems were based on the CIGRE LV European distribution network benchmark, and was implemented into DIgSILENT PowerFactory to run load flow calculations, on different cases. In the different cases, properties of the PI controller, the power lines, and the loads were varied. After running all simulations, the performance of the controller for each case could be judged against criteria which were decided upon, to determine if the performance was feasible or not, along with stability of the controller.

After analysing the performance in all cases, whether or not the controller was feasible seemed to be related to the loop gain of the entire system. This in turn seemed to be proportional to the number of PV units installed, the resistance in the system, the proportional gain of the PI controller, as well as inverse proportional to the integrating time constant of the PI controller. The loads did not affect the feasibility of the system.

Keywords: distributed generation, active network management, low voltage distribution network, delta control, voltage control

Preface

Finally, my turn has come, to present my master's thesis, and finish my time at LTH. It took a bit longer than I had first anticipated, and there were quite a few hurdles along the ride, but now I too can call myself an engineer. I think this thesis is truly representative of what these years have looked like; curiosity, some insecurity, several sidetracks, but most importantly, an enormous gratitude for every opportunity that has crossed my path.

Speaking of gratitude, I would like to extend my thanks to my supervisors, Olof Samuelsson and Martin Lundberg. You gave me this opportunity, and helped me through all my confusion and sidetracks, and eventually there was actually work that could be presented. Your feedback, guidance, and your trust in me has truly been invaluable. I would also like to thank the rest of the staff at IEA, for helping me with various issues, making me feel at home at the division, and of course, for opening the door to the lunchroom for me.

I would finally like to thank my friends. I think the best thing to come out of this education is our friendship. Studying together, laughing together, crying together. You believed in me when i didn't, and I truly wouldn't have come this far without you. Everybody deserves friends like you.

Charlotta Sporre
Lund, January 2024

List of abbreviations

ANM - Active network management
DG - Distributed generation
DN - Distribution network
DSO - Distribution system operator
HV - High voltage
LV - Low voltage
MV - Medium voltage
PF - DIgSILENT PowerFactory
PI - Proportional integrating
PV - Photovoltaic
TN - Transmission network

Contents

Chapter 1

Introduction

In this first chapter, the problem of this thesis is introduced, along with a short background to the issue at hand. In the later part of this chapter, the objectives of the thesis are presented, as well as the scope and delimitations.

1.1 Background

Electric power distribution systems are traditionally designed to supply consumers with electricity. As more households are installing solar panels, and becoming both consumers and producers of electricity, the distribution network also has to be able to receive electricity from household producers. When more photovoltaic (PV) power production is connected to a system, there is an increased risk of bottlenecks, overloaded power lines and transformers, and overvoltages [1], the last of which is going to be the main focus in this thesis. Overvoltage can cause issues to the consumer, in the form of excess tear of any electronics plugged in to the network. Because of this, there are guidelines nationally regarding what voltages are allowed [2].

The most common method to reduce the risk of overvoltage is to expand and reinforce the network [1, 3]. Another method, which is what this thesis is going to evaluate, is to actively control the components causing the issue. The concept of actively controlling the components of the network is called active network management (ANM), and is a stark contrast to the conventional passive methods of managing the grid. This can be done by locally controlling active and reactive power in the converter of the PV units. However, by controlling the active power injected by the PV units, it will also result in a loss of income for the producer [4], which is why it is often more preferable to control the reactive power. This can reduce the voltage increase from the PV units, without affecting the income for the owner. Controlling the reactive power does however have a limited effect on the voltage, especially in the low voltage distribution network [5], which is why control of the active power might eventually also be needed.

A fairly simple and low-cost way to go about this is by implementing so called plug-and-play, where each node is locally controlled by a PI controlled PV converter, all of which are tuned the same. In a radial distribution network, the feeder expand radially from the transformer, with cables branching off along the feeder. In such a network, the nodes furthest from the transformer will experience the highest voltage increase to the network [6]. Thus it would seem most effective to suggest countermeasures in the periphery of the network. A drawback from local control of the converters however is that the resources at hand might

not be used in the most effective way possible. Local control is also unfair, as it is most disadvantageous to the producers at the end of the feeder, resulting in a loss of revenue. To minimise the loss of revenue in one spot, and to use the resources more efficiently, it could be advantageous to spread out the control across the network.

In this new interconnected system of several local PI controllers, stability of the entire system still needs to be ensured. Analytical proof of this stability has been achieved [7], but only demonstrated for a small and generic system. In order to properly ensure the stability of this control method, the size and topology of this test system would need to be altered, and the stability of the control method would be assessed for these new configurations.

1.2 Problem Statement and Aim of Research

An increasing amount of distributed generation (DG) in the distribution network (DN) results in power flows in the network no longer being able to be assumed unidirectional. The aim of this thesis is to find and test a method of active network management (ANM), which would counteract some of the issues caused by this shift of power flow.

One such ANM method has been developed [7], where a system of local PI controllers within each converter is used to control voltages in the nodes throughout the feeder. The aim of the research in this thesis is to study how this method could be used in different systems, with different physical properties. By preforming simulations of a test system, equipped with the ANM control method, the aim is to find how these physical properties, along with the properties of the PI controllers, affect the stability of the entire system. In order to study this, the simulations will be run on test systems where one parameter is changed at one time. The aim is to find both how physical properties of the DN and properties of the PI controllers affect the stability and performance of the system. Throughout the different simulations, three aspects of the system are studied; the controller parameters, the physical properties of the power lines of the system, and the loads connected to the nodes of the system.

1.3 Objectives

The objectives of this thesis is as follows:

- Find a test system, and make any necessary alterations, which can be used to run the simulations in DIgSILENT PowerFactory.
- Implement a Python script, fitted to the test system, which can apply the ANM algorithm to the simulations.
- Find a base case where the system is stable and preforming in a desirable manner, which can later be built upon to create new test cases.
- Implement a method to vary the parameters being studied, and create test cases where one parameter is being changed at one time.
- Find a method to systematically categorise the performance of the system in each test case.
- Assess how the different parameters affect the stability and performance of the system.

1.4 Scope and Delimitations

The scope of this thesis is to assess the performance of the ANM algorithm established in [7] when implemented in test systems with varying physical properties, and different controller parameters. With this, the hope is to find a relationship between these properties and the performance of the system.

In order to carry out this research, a few delimitations have to be established. First, this thesis will only study how the algorithm is able to control the voltage of the nodes, and congestion management is out of scope. Second, there are several different types of DG upon which the algorithm could be applied. In this thesis, only photovoltaic (PV) cells will be used as a power source to be controlled. Third, there are several different voltage levels to the DN where the algorithm could be implemented. In order to study how the algorithm could affect households producing their own PV power, this thesis considers low voltage (400 V), residential, radial distribution networks only. Finally, there is a large number of parameters to choose from when varying the system. When studying how the algorithm functions, it was decided that the most interesting parameters would be the proportional gain (K) and integrating time constant (T_i) of the PI controller, the length and resistance (R) of the power lines, and the active (P) and reactive (Q) power absorbed by any load connected to the nodes.

Chapter 2

Theory and Tools

In order to understand the problem this thesis is trying to study, some background of the issues are needed. This chapter is aiming to give some context to what distributed generation in a low voltage distribution network looks like, as well as issues that may arise from it. Next, the theory behind the tools used throughout this thesis will be presented.

2.1 Low Voltage Distribution Networks

In order to deliver electricity from producer to consumer, it is transported via the power grid. The power grid is divided into different levels with different voltage levels. In Sweden, the two main levels are the transmission and the distribution network [8]. The transmission network (TN) is the highest level, with the highest voltage. In Sweden, the voltage in the TN is either 400 or 220 kV [8]. Traditionally, this is where all the power is injected into the network, and is where all the large power plants are connected. The next level is the distribution network (DN). In Sweden, the DN has voltage levels between 130 kV all the way down to 400 V line-to-line (230 V line-to-neutral) at the consumer [8]. Traditionally the DN is only used to deliver power from the TN to the consumer. Thus, during planning of the DN, unidirectional power flow could be assumed, i.e. that the power would always be flowing from the higher voltage levels to the loads at the lower voltage levels. [6]

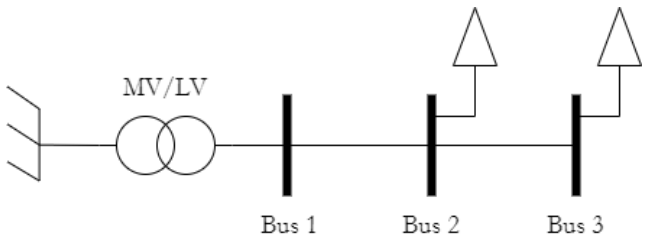

Figure 2.1: Single line diagram of a radial low voltage distribution network, with a MV/LV transformer, three buses, and two loads connected.

In the low voltage (LV) part of the DN, i.e. the level closest to the consumer (400 V), the network is dimensioned to deliver power from the MV/LV substation radially to the load, with several loads on each feeder, in the form of consumers being connected to the grid, see

figure 2.1. As the power flows past each load, the voltage gets progressively lower, leading to the highest voltage at the substation, and the lowest voltage at the load furthest from the substation [9]. In order to ensure that the voltage is still at an adequate level at the end of the feeder, the voltage at the head of the feeder is set to slightly higher than nominal voltage. The voltage at the MV/LV substation is set with a tap changer. By setting the voltage higher than nominal at the substation, the voltage is ensured to stay over the lower limit of the network, even during peak load [6].

2.1.1 Voltage Sensitivity to Active and Reactive Power

As power flows in the DN, it will affect the voltage in the nodes along the feeder. How it affects the magnitude of the voltage can be described as the nodes *voltage sensitivity* [6]. The voltage can be interpreted as a function of the active and the reactive part of the power:

$$V = f(P, Q) \tag{2.1}$$

Thus a change in power will affect the voltage as:

$$dV = \frac{\partial V}{\partial P} dP + \frac{\partial V}{\partial Q} dQ \tag{2.2}$$

where $\frac{\partial V}{\partial P}$ and $\frac{\partial V}{\partial Q}$ is the voltage sensitivity to variations in active and reactive power respectively. In order to get an understanding of this sensitivity, it can be exemplified with a Thévenin equivalent (figure 2.2) consisting of a source voltage ($\mathbf{V}_{Th}$), a line impedance ($\mathbf{Z}$), a load absorbing the apparent power $\mathbf{S}$ with the receiving voltage $\mathbf{V}_r$ across it, along with the current $\mathbf{I}_{Th}$ running through the circuit. It should be noted that any term in **bold** should be regarded as a phasor, with any corresponding phasor angle presented in figure 2.2.

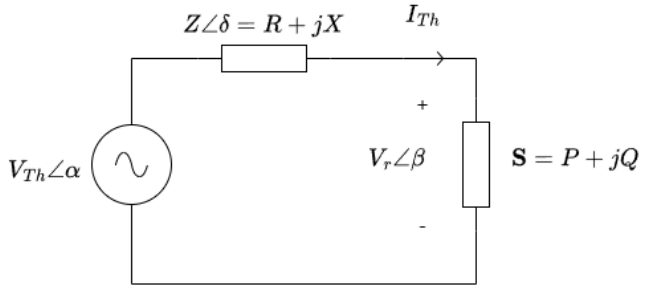

Figure 2.2: Thévenin equivalent used to determine voltage sensitivity to variations in active ($\frac{\partial V}{\partial P}$) and reactive ($\frac{\partial V}{\partial Q}$) power. The circuit consists of the source (Thévenin) voltage, $\mathbf{V}_{Th}$, line impedance, $\mathbf{Z}$, apparent load, $\mathbf{S}$, with the receiving voltage, $\mathbf{V}_r$, and current $\mathbf{I}_{Th}$

The apparent power absorbed by the load is described as:

$$\mathbf{S} = \mathbf{V}_{Th} \cdot \mathbf{I}_{Th}^{*} \tag{2.3}$$

Using Ohms law we can rewrite the apparent power as:

$$\mathbf{S} = \mathbf{V}_{Th} \cdot \left(\frac{\mathbf{V}_{Th} - \mathbf{V}_r}{\mathbf{Z}} \right)^{*} \tag{2.4}$$

$$\mathbf{S} = V_{Th}e^{j\alpha} \cdot \left(\frac{V_{Th}e^{j\alpha} - V_r e^{j\beta}}{Ze^{j\delta}}\right)^* \tag{2.5}$$

$$\mathbf{S} = \frac{V_{Th}^2}{Z}e^{j\delta} - \frac{V_{Th}V_r}{Z}e^{j(\alpha-\beta+\delta)} \tag{2.6}$$

Equation 2.6 shows the apparent power received by the load. The apparent power consists of the active power, P, which corresponds to the real part of the apparent power, and the reactive power, Q, which is the imaginary part. Similarly, the impedance consists of a resistance, R, and a reactance, X, with $\delta = arctan\frac{X}{R}$ being the angle between R and X. Thus, we can conclude:

$$P = \frac{V_{Th}^2}{\sqrt{R^2+X^2}}cos(arctan\frac{X}{R}) - \frac{V_{Th}V_r}{\sqrt{R^2+X^2}}cos(\alpha-\beta+arctan\frac{X}{R}) \tag{2.7}$$

$$Q = \frac{V_{Th}^2}{\sqrt{R^2+X^2}}sin(arctan\frac{X}{R}) - \frac{V_{Th}V_r}{\sqrt{R^2+X^2}}sin(\alpha-\beta+arctan\frac{X}{R}) \tag{2.8}$$

In a DN, the angle between the sending voltage (here $\mathbf{V}_{Th}$) and receiving voltage ($\mathbf{V}_r$) is small [9], and thus it can be assumed that $\alpha - \beta \approx 0$. Using this assumption in equations 2.7 and 2.8 we obtain:

$$P = \frac{V_{Th}^2}{\sqrt{R^2+X^2}}cos(arctan\frac{X}{R}) - \frac{V_{Th}V_r}{\sqrt{R^2+X^2}}cos(arctan\frac{X}{R}) \tag{2.9}$$

$$Q = \frac{V_{Th}^2}{\sqrt{R^2+X^2}}sin(arctan\frac{X}{R}) - \frac{V_{Th}V_r}{\sqrt{R^2+X^2}}sin(arctan\frac{X}{R}) \tag{2.10}$$

In order to study how the power affect the voltage, the partial derivatives of equation 2.9 and 2.10, with respect to V_r, are computed:

$$\frac{\partial P}{\partial V} = -\frac{V_{Th}}{\sqrt{R^2+X^2}}cos(arctan\frac{X}{R}) = \left(\frac{\partial V}{\partial P}\right)^{-1} \tag{2.11}$$

$$\frac{\partial Q}{\partial V} = -\frac{V_{Th}}{\sqrt{R^2+X^2}}sin(arctan\frac{X}{R}) = \left(\frac{\partial V}{\partial Q}\right)^{-1} \tag{2.12}$$

Now, equation 2.11 and 2.12 can be used to study how the R/X ratio will affect the voltage of a node. If $R >> X$:

$$\frac{X}{R} \to 0 \;\Rightarrow\; arctan\frac{X}{R} \to 0 \;\Rightarrow\; sin(arctan\frac{X}{R}) \to 0,\; cos(arctan\frac{X}{R}) \to 1$$

and

$$\sqrt{R^2+X^2} \to R$$

resulting in:

$$\frac{\partial V}{\partial P} \to \frac{R}{V_{Th}},\; \frac{\partial V}{\partial Q} \to 0 \tag{2.13}$$

Using the same logic for $X >> R$ results in:

$$\frac{\partial V}{\partial Q} \to \frac{X}{V_{Th}},\; \frac{\partial V}{\partial P} \to 0 \tag{2.14}$$

From equation 2.13 and 2.14, the conclusion can be drawn that for large values of R/X, the active power will have a greater effect on the voltage, and for small values of R/X, the reactive power will have a larger effect on the voltage.

2.1.2 Distributed Generation in Low Voltage Networks

As more consumers install distributed generation (DG), e.g. solar cells which are the focus of this thesis, the power flow in the DN can no longer be assumed to be unidirectional [10]. As the power produced by the DG in a node exceed that of the load, the power will instead be injected into the DN. This will in turn increase the voltage in said node, which will affect the voltage across the feeder.

Setting the voltage at the transformer higher than nominal will protect the DN from reaching too low voltages. However, when the voltage is set above nominal, there is little room left for voltage increase from DG. This heavily limits the possibility of injection from renewable power sources. As long as there is only limited number of DG units connected to the feeder, there will not be enough power production to heavily affect the voltage across the feeder, and the margins are still sufficient to manage a voltage increase. However, when the number of units increase, so does the effect of the accumulated power production on the voltage of the feeder. As was depicted in equation 2.2, an increase in power will result in an increase in voltage. If the installed power become too great, the voltage margins might not be enough to protect the DN from overvoltage. Figure 2.3 show that a higher than nominal voltage will result in large margins when having loads connected, but a much smaller margin when there is a lot of generation connected. Furthermore, just as how the voltage decreased the most at the end of the feeder, if all nodes become producers, the highest voltage increase occurs here as well, thus punishing any DG at the end of the feeder. [6]

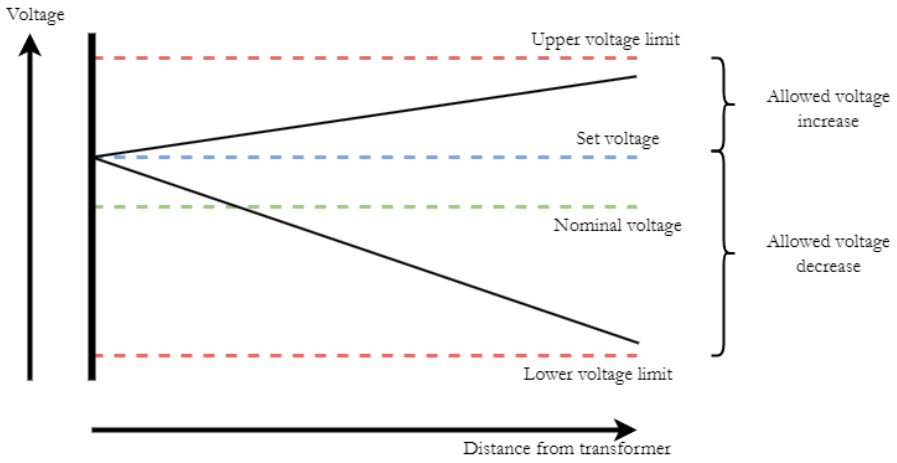

Figure 2.3: Voltage profile along feeder when having either generation (upper solid line) or loads (lower solid line) connected, and the voltage at the transformer is set higher than nominal.

Today, this issue is managed by the DSO by reinforcing the DN [3]. By increasing the capacity of the transformers, or installing more or larger cables, the margins for the voltage in the DN increase. However, not only is this very costly for the DSO, but it will also stall any new installation of DG. If the DSO cannot guarantee adequate voltage quality when if new DG is installed, it will not be allowed. Thus any potential new producer will have to wait until the network is reinforced, and has the capacity for more DG.

2.2 Overvoltage

As previously stated, overvoltages are expected to become a larger issue as more renewable DG is installed in the DN.

The purpose of avoiding overvoltages is to ensure the voltage quality of the power that reaches the consumer, ensuring the consumer in question can feel secure in knowing what they plug their equipment into. If the voltage diverges from the acceptable interval, either above or below the limits, it can cause issues for any electronics plugged in to the voltage source.

If the voltage is greater than the interval allows, it will cause an increased current, which in turn can cause excessive wear of the equipment connected to the voltage. If instead the voltage drops below the lower limit, it can cause the equipment to function ineffectively, and sometimes not to function at all.

Thus, it is the DSO's responsibility to keep their voltage within these limits. The limits are set according to governmental regulations in each country. In Sweden, this falls upon Energimarknadsinspektionen, the Swedish Energy Markets Inspectorate (Ei). According to Ei [2], for reference voltages up to 1000 V, the maximum voltage allowed is 1.35 p.u.. The voltage is also not allowed to rise above 1.15 p.u. for more than 5 s. Ei also declare that any voltages that exceed 1.11 p.u. for more than 200 ms need to be resolved in a way that the means seem reasonable according to the situation. These limits are also presented in table 2.1.

Table 2.1: Voltage limits for short term voltage rises, as established by Energimarknadsinspektionen, Ei [2]. Voltages within area A are deemed adequate. Voltages within area B should be resolved in a way so that the means seem reasonable according to the situation. Voltages within area C are not allowed.

Nodal voltage, V [p.u.]	Duration, t [ms]		
	$10 \leq t \leq 200$	$200 < t \leq 5000$	$5000 < t \leq 60000$
V≥1.35	C	C	C
1.35>V≥1.15	B	B	C
1.15>V≥1.11	A	B	C
1.11>V≥1.10	A	A	A

2.3 Active Network Management

When DG, in the form of PV units, is installed, the power produced is inherently unpredictable. This will lead to the net power of the node, consisting of power drawn by any load and power injected by any DG, being unpredictable as well. If the PV production is high, while the loads are low, any excess power will be injected into the DN, which cause the voltage to rise [10]. As mentioned in section 2.1.2, today this unpredictability of the load flow is handled by reinforcing the DN. What this thesis want to explore is instead the possibility of implementing active network management (ANM) in order to control the power flowing in and out of the nodes.

ANM is an alternative strategy to the conventional "fit-and-forget" strategy of designing power distribution systems. The conventional DN is designed to deliver power from the TN to the consumer, and operate without a need for control. By instead implementing an ANM method to the network, it unlocks the possibility to avoid congestion, overloading, and overvoltage [11, 12]. Different methods of control can be used when implementing ANM,

e.g. controlling transformer taps, system reconfiguration, and active and reactive power management [11], the latter of which is the method used in this thesis. This would reduce the need for conventional network reinforcement, the waiting time for connecting new DG to the DN, and the cost for the consumers connected to the DN [12].

2.3.1 Local Control Strategies

ANM takes advantage of the ability to control the converters in converter based DG. The converters could thus be controlled with PI controllers, which is what the algorithm used here is implementing. This makes it so that the network can be controlled without having to add extensive infrastructure, such as communication, to the DN. By implementing so called "plug-and-play" solutions - i.e. identical parameter settings for all the controllers in the system - there is also little to no need for reconfiguration of the network controllers as units are added or removed.

The purpose of implementing such a solution would be, as stated earlier, to avoid over-voltages, by reducing the voltage in the node if it becomes too large. By taking advantage of the converters of the DG, the voltage can be measured and compared to a reference value of the voltage. If the voltage is deemed too large, the power from the DG could be curtailed in order to reduce the voltage back down. However, if the voltage is still within an acceptable interval, there is no need for any curtailment, and the controller should thus not be activated. This calls for a one-sided (i.e. only active if the voltage exceed a set limit), discrete PI controller to be used in the converters of the system.

The ANM algorithm used in this thesis [7] takes advantage of three different types of decentralised voltage control. *Supporting strategies* aim to reduce the voltage increase while still within acceptable levels. *Set point tracking strategies* are used to ensure that the voltage follows predetermined reference signals. *Limitation strategies* act as disturbance rejection, and is restricted to only act when violations of the preset constrains occur.

2.3.2 Controlling PV Power

When controlling voltage levels, varying both active (P) and reactive (Q) power will impact the voltage. Traditionally, when implementing converter based voltage control, controlling Q is preferred, due to curtailment of P will result in reduced revenue [4]. However, the effectiveness of using either P or Q to control the voltage will depend on the ratio between resistance (R) and reactance (X) of the lines in the network. In a HV network, the R/X ratio is usually very small. Thus controlling Q will have a large impact on the voltage in the network, see equation 2.12. On the contrary, in a LV network, the R/X ratio is usually much larger, meaning that controlling Q will not be as effective when managing the voltage [5]. In a LV network, the R/X-ratio is typically in the range of 0.70 - 11.00 [13], meaning that potentially P could be 11 times as effective in controlling the voltage as Q. This shows that despite the potential revenue losses brought on by decreasing the active power, there still might be advantages to using P to control the voltage levels.

If the voltage in a node exceed the determined maximum voltage allowed, it will first be reduced by a constant power factor ($cos\varphi$) control scheme. This control scheme works by estimating the maximum allowed Q output based on the voltage in the node and $cos\varphi$. If needed, the PV unit is drawing reactive power from the grid, reducing the voltage in the process [14]. If the voltage is still above maximum, and the PV unit cannot draw more reactive power, there exists a need to reduce the active power as well.

If implementing a way to estimate the maximum active power generation in a PV unit

[7], this estimated power generation can then be used to set a reference value for a local controller. This type of control, so called delta control, use a set point active power injection (p^{gen}), and the estimated maximum power injection ($\tilde{p}^{gen}$), to produce the delta control signal (δp^{gen}):

$$p^{gen} = \tilde{p}^{gen} + \delta p^{gen} \tag{2.15}$$

Here the delta control signal $\delta p^{gen} \leq 0$, since the active power injection p^{gen} cannot be larger than the maximum power injection $\tilde{p}^{gen}$.

2.3.3 Local PI Control

In order to implement delta control, the delta control signal will be used in a linear, discrete time, single-input-single-output (SISO) PI controller with zero-order hold integration. The general version of this PI controller can be written as in eq. 2.16.

$$u(t_k) = u(t_{k-1}) + K\Big(\Big(1 + \frac{T}{T_i}\Big)\, e(t_k) - e(t_{k-1})\Big) \tag{2.16}$$

Here, t_k is the current time step, u is the output, e is the input, or error signal, T is the sampling interval, and K and T_i are the PI design parameters. In order to apply this general PI controller to the delta control model from equation 2.15, the model is expanded to include several parallel PI controllers. This is done by defining for each DG unit l, $u_l = \delta p_l^{gen}$, $e_l = v_l^{ref} - v_l$, where $v_l^{ref} = v_{grid,l}^{max}$ is the constant maximum voltage in the grid, ensuring curtailment in the case of overvoltage. The different controllers are assumed to be tuned identically according to plug-and-play. The multiple parallel PI controllers can be described as:

$$\delta \mathbf{p}^{gen}(t_k) = \delta \mathbf{p}^{gen}(t_{k-1}) - K\Big(\Big(1 + \frac{T}{T_i}\Big)\mathbf{v}(t_k) - \mathbf{v}(t_{k-1})\Big) + K\frac{T}{T_i}\mathbf{v}_{grid}^{max} \tag{2.17}$$

where $\delta \mathbf{p}^{gen}$ and $\mathbf{v}$ are vectors containing the values for all DG units l.

2.3.4 Anti-windup

Due to physical limitations of the PV units, there will also be limitations to the operational ranges of the PI controllers. If the voltage in a node is below the upper limit, the controller will try to increase the output of the DG. This, however, is not possible unless any active power has previously been curtailed. On the other hand, it is not possible to curtail more power than is being generated by the DG. Thus, in eq. 2.17 the following limits are applied:

$$0 \leq p_l^{gen} \leq \tilde{p}_l^{gen} \tag{2.18}$$

or equivalently:

$$-\tilde{p}_l^{gen} \leq \delta p_l^{gen} \leq 0 \tag{2.19}$$

However, issues can occur when the desired output lies beyond these limits. Going back to the general controller in equation 2.16, if $u(t_k)$ is saturated to either limit, the integrator will continue accumulating the error $e(t_k) - e(t_{k-1})$. Let this accumulated error, while the output is saturated, be called e_{sat}. When the input later pass the reference value, the error

$e(t_k)$ will change sign. Despite this, e_{sat} will be so large that it will counteract this sign change, and the output will remain saturated, resulting in a much slower controller. This phenomenon is known as an integrator windup [15], and can be resolved by ensuring $e_{sat} = 0$ at all times. The way this is done is simply by recognising whether $u(t_k)$ is saturated, and if it is, let $e(t_k) = 0$, meaning no error will be accumulated when the output is saturated.

2.3.5 System Stability

In equation 2.17 the controller has been established, along with the physical limitations of the delta control signal in equation 2.19. This controller can now be applied to a power grid, according to the block diagram in figure 2.4.

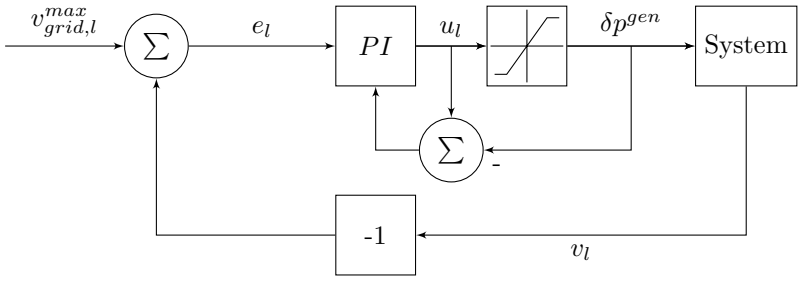

Figure 2.4: Block diagram of a PI controller in a DG unit l connected to a test system. v_l is the measured voltage in the node, and is compared to the maximum allowed voltage $v_{grid,l}^{max}$. The difference, e_l, is used as an input in the PI controller (see equation 2.17), which produce an output u_l. The saturation limits from equation 2.19 is applied to the output, and the control signal δp_l^{gen} can be used on the system. The output before and after the saturation limits are compared to one another. If these differ, the integrator will be limited according to the anti-windup method from section 2.3.4.

For each node where a PV unit is connected, there is a PI controller associated with it. Thus, every node is now a closed loop system, where the controller is determining the power output from the node, and in turn controlling the voltage of the node. When applying the delta control scheme to a system of nodes in a grid, not only will the controllers affect each other, but there is now physical aspects of the grid which will affect the controllers as well. These physical properties of the grid is represented in the block scheme as the voltage sensitivity of each respective node, as discussed in section 2.1.1. Equations 2.11 and 2.12 shows that the determining factor of the voltage sensitivity is the impedance of the DN. Thus in order to achieve stability throughout the system, the impedance need to be taken into consideration, in addition to the parameters of the controllers themselves.

Furthermore, due to the physical limits of the PV units, and the anti-windup scheme implemented, the linearity of the controller will be affected as it reaches the saturated levels. Thus, these saturation limits will also affect the stability of the entire system.

When applying the discrete PI controller to a system, an appropriate sampling interval (T in equation 2.17) has to be decided on. When running a simulation of the system, a load flow calculation is run over the determined sampling interval. Thus, during the calculation the system is assumed to be static. When studying fast voltage variations due to power variations, the system can be assumed static in the interval $10^0 - 10^3$ s [16]. Thus, T has to be somewhere in this interval to run load flow calculations on a static system.

While this thesis will focus on finding stable systems through numerical solutions to the problem, an analytical approach to the stability problem have been developed [7]. By studying the eigenvalues of the complete system around an operating point, it can be shown that in an arbitrary radial DN it is possible to find a stable equilibrium. This analytical approach can be used in order to determine whether a controller is stable or not. However, it does not tell anything else about the behaviour of the controller. This is why this thesis is focused on the numerical approach to the problem, where the controller can be implemented on different test systems, and the performance be analysed.

2.4 CIGRE LV Benchmark

In order to test the controller, it is implemented in a test system that reflects the conditions of a real DN. Thus, for this thesis, the CIGRE LV distribution network benchmark [13] has been used.

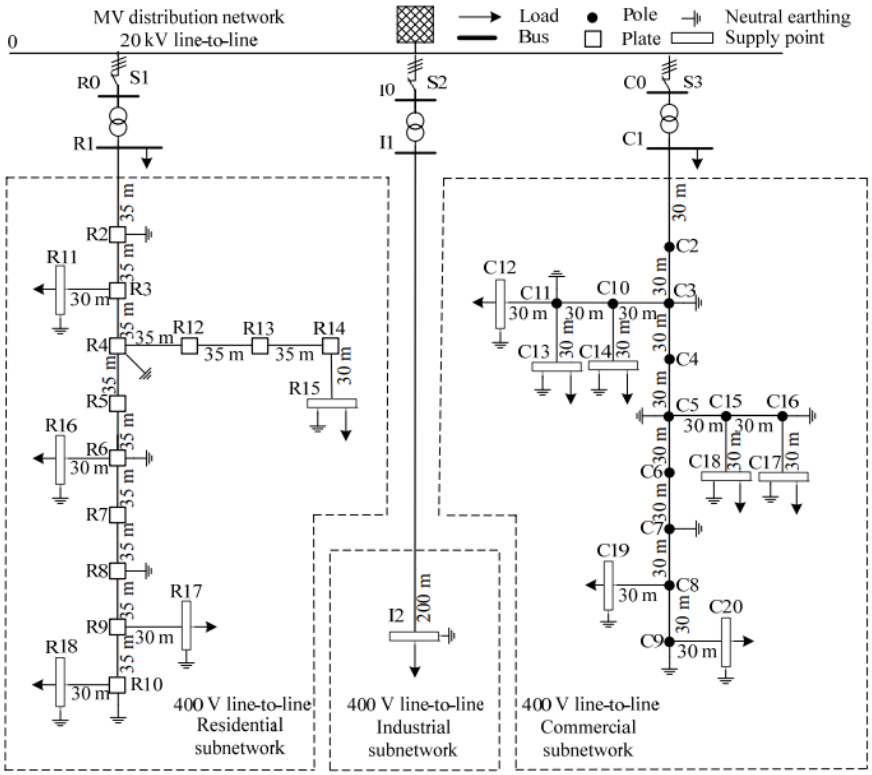

Figure 2.5: Single line diagram of the CIGRE European LV DN benchmark [13].

2.4.1 Configuration

The CIGRE LV DN benchmark is available for two different configurations, North American and European. In order to simulate conditions in Sweden, the European network is chosen.

The network is radial in structure, with a MV/LV transformer at the start of the radial.

The network consists of three subnetworks, see figure 2.5, in order to reflect residential, commercial, and industrial sectors. Each subnetwork is equipped with its own transformer, and a one feeder expanding radially from the transformer. In this thesis, only the residential subnetwork will be used.

2.4.2 Network Data

Since only the residential subnetwork is used, from here on only data relevant to this subnetwork will be discussed.

The residential subnetwork is modeled to be an urban area, thus only underground (UG) cables are used. In table 2.2 relevant data for the line types used are presented. Note that these line types are the original ones used in the CIGRE network. During simulations, some parameters may be varied. The two different line types, UG1 and UG3, is used in different parts of the subnetwork. The less resistive line type, UG1, is used in the main radial of the feeder, from R1 all the way to R10. UG3 is instead used where the feeder branches off to the supply points (R3-R11, R4-R15, R6-R16, R9-R17, R10-R18).

Table 2.2: Line types used in the residential subnetwork with corresponding resistance and reactance, and the resulting R/X ratio [13]. Note that there are more line types used in the rest of the benchmark, but given the fact that only the residential subnetwork has been used throughout this thesis, only the line types used in this subnetwork are displayed.

Line ID	Resistance, R [Ω/km]	Reactance, X [Ω/km]	R/X
UG1	0.162	0.074	2.2
UG3	0.822	0.078	10.5

The residential subnetwork consists of 18 nodes in total, R1 - R18. The first of these nodes, R1, is the bus where the feeder is connected to the transformer. At this bus there is one load connected, LR1, and is originally set to 200 kVA. This is meant to represent other feeders that may be connected to the transformer. Five nodes are so called supply points - nodes R11, R15, R16, R17, and R18 - and represent one, or a group of houses. Originally these nodes each have one connected load. However, since this thesis is meant to study the effect of DG on a LV DN, at each node a PV unit is also connected. The rated power for these units, as for each of the loads, will vary throughout the different cases, and thus the power for each unit will be presented during each case.

The transformer used in the subnetwork is a MV/LV transformer, with $V_1 = 20$ kV, and $V_2 = 0.4$ kV. The transformer is rated for 500 kVA, meaning the max allowed load/power production is 500 kVA.

Chapter 3

Methodology

In the previous chapter, the background to the problem has been established, as well as an explanation to the tools used. This chapter aims to explain how the tools were implemented, as well as establishing how the practical work of the thesis were carried out.

3.1 Implementing Active Network Management

In order to study the ANM algoritm, it was used along with simulations run in DIgSILENT PowerFactory (PF). PF is a program used for simulations of power systems. By creating a test system, with certain initial values, the program can run iterative load flow calculations on the system. The length of each iteration is based on the sampling interval of the PI controller, which has to be set so that the system is assumed static, as discussed in section 2.3.5. In order to have quite fast controllers, this is set to $T = 3$ s. PF also has the ability to be run externally via Python scripts. Thus, in order to implement the ANM algorithm, this was done so in a Python script, which in turn could run load flows in PF.

The first step to be able to run the simulations was to implement the CIGRE LV benchmark into PF. This was already available at the department, and was provided for this thesis. Minor changes to the benchmark needed to be done, by connecting PV units to each of the supply nodes in the residential subnetwork. In order to run the ANM algorithm on the test system, a script developed by Martin Lundberg was provided as well. This script had implemented the controller described in section 2.3, so that it was compatible with PF simulations. In order to have the script work for the CIGRE LV benchmark, certain adjustments had to be done to the script as well.

When the script is run, the initial values, as well as the length of the simulation, is defined in the script. The initial values are used to calculate appropriate control signals within the script. The determined control signals are sent to PF, which runs a load flow calculation with the given values. The results of the load flow are sent back to the script as new inputs in the controller. The new inputs are used to determine outputs for the next time step, which are sent to PF, and so on. This loop is continued for as many time steps which was defined in the script before the simulation was run.

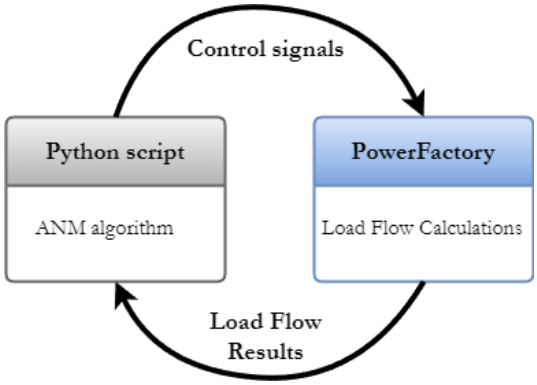

Figure 3.1: Flow chart of the communication between the script running the ANM calculations, and PowerFactory running load flow calculations, and taking a time step T in between each cycle.

3.2 Determining Stability and Feasibility of the System

When determining the stability of the system, the step response of the controller is analysed. The simplest way of determining whether the controller is stable or not, is by studying any potential oscillations in the step response. If there are no oscillations in the step response, or if the oscillations die down, the controller can be ruled as stable. If, however, the oscillations remain constant, or increase in amplitude, the controller is determined to be unstable.

The next step is to determine whether the controller, in the given system, is functioning within acceptable ranges. In this thesis, this property of the controller will be referred to as *feasible performance*. The feasibility of a controller in a given case is determined by analysing the results of the step response. The controller is implemented to control overvoltages in a DN. Thus the step response has to be analysed according to two general performance criteria:

- The controller is able to regulate the voltage down before it exceeds a determined maximum voltage level.
- The controller is able to regulate the voltage down to a decided voltage level within a reasonable amount of time.

These criteria does however raise a few questions. First, what is the determined maximum voltage level? And second, what is considered to be a reasonable amount of time? Since the controller is implemented in a LV DN, the step response has to be analysed from the perspective of a DSO, which have to keep the voltage quality within acceptable levels. For this there is documentation specific for each country, see the section 2.2 above. In order to adhere to Swedish standards for voltage quality, the voltage has to fall within the limits set by Ei (see table 2.1).

These regulations will give hard limits that the controller have to adhere to. However, to determine whether the controller could actually be suggested as a feasible one, it will in this thesis also be subject to set *feasibility criteria*. These criteria are concrete versions of the general criteria stated above. First, the determined absolute maximum voltage that is allowed will be set to 1.35 p.u., in accordance to the Swedish regulations. Furthermore, the

controller will have to be able to push down the voltage in such a time that it is still within the limits set in table 2.1.

Second, a reference voltage has to be set for the controller. This is the voltage level at which the controller will kick in, as well as the voltage level that the voltage in the node is supposed to stabilise at. In equation 2.17, this is denoted as $\mathbf{v}_{grid}^{max}$, and will be set to 1.05 p.u. during the simulations. The reason this is set as the reference for the controller is that is far enough from any limits given by Ei. It is also far enough above nominal voltage that it provides room for a fair amount of power output from the node. Furthermore, there has to be a time for the voltage to be reduced back to the reference voltage, that is determined to be reasonable in order to judge the controller as feasible. In order to ensure that the voltage returns to to the reference voltage during the simulation time, and in order to not have to run simulations over a too long time, this limit is set to 90 s. This also ensures that the voltage returns to a stable level in a short enough time so that other properties of the system do not change, such as increase in solar irradiation, higher or lower loads etc.

The last aspect to consider, is any potential oscillations in the voltage levels. Even if the system is stable, and does return to the reference voltage at some point, there might still be oscillations in the voltage which could be disruptive. While these oscillations are not desirable, it could also be to strict of a criterion to not allow for any oscillations. In order to ensure that these potential oscillations are dampened in a timely manner, they have to be reduced by 90% within 30 s in order to be determined feasible.

To summarise, the feasibility criteria are as follows:

- **Criterion 1:** The controllers in the system must behave in a stable manner.
- **Criterion 2:** The voltage in any given node may not exceed any limits set by Ei, see table 2.1.
- **Criterion 3:** The voltage in any given node has to be stable at 1.05 p.u. no more than 90 s after the controller is activated.
- **Criterion 4:** Any oscillations that occur in the voltage at any given node has to be reduced in amplitude by 90% no more than 30 s after the controller is activated.

3.3 Base Case

In order to ensure that the controller method works, even in a very simple setup, a base case is created in the CIGRE LV network. This base case will later on work as a foundation, that all other cases are built upon.

Throughout the simulations run in this thesis, only one or two supply points will have any installed PV units or loads. The power produced in the PV is purely active, i.e. $cos\varphi = 1$. In the base case, there is only production, and no load, installed in the supply points, see table 3.1a and 3.1b, and no other feeders are connected to the transformer (i.e. no load in node R1). When using two supply points, the installed PV in R17 and R18 are of the same size. The nodes are chosen due to their location. R17 and R18 are placed furthest away from the transformer, and thus any production that occurs here will have the largest effect on the voltage at R1.

Table 3.1: Loads and installed PV during the base case simulations for one and two installed PV units.

(a) Network data during base case using one PV unit.

Node	Installed PV [kW]	Load [kVA]
R1	N/A	0
R11	0	0
R15	0	0
R16	0	0
R17	0	0
R18	200	0

(b) Network data during base case using two PV units.

Node	Installed PV [kVA]	Load [kVA]
R1	N/A	0
R11	0	0
R15	0	0
R16	0	0
R17	200	0
R18	200	0

In order to see how the controller react to changes in power production, a step in generation was set from 0% to 100% of installed capacity after 9 s. As the power injection from the PV in the nodes increase, so will the voltage. The controller will however not start controlling the power injection until the voltage exceed a determined reference voltage. Thus, in order to judge the stability of the controller, it is essential that the voltage exceed this reference. The simulation is then run for 120 s after the step in production, and the resulting step response can be used to determine the stability of the system.

3.4 Varying System Parameters

In order to study how the controllers perform in different situations, it is also necessary to study the controllers in different LV systems. Thus, a few different parameters were chosen to be varied during different simulations. For each system, the base case was used as a template, and the new system was created by varying the chosen parameter. In each of these simulations, the stability of each respective step response could be determined. For this, three different aspects of the system was determined to be varied; the controller itself, the power lines in the system, and the loads connected at the nodes. The first aspect, the controller parameters, was chosen to be varied in order to study in what interval the parameters would yield a controller that could still be used, when it would be deemed too slow, and when it would reach instability. The next aspect, the power lines, was chosen to be varied in order to study how the impedance in the system would affect the feasibility of the system. Increasing the length or the resistance of the power lines will both increase the impedance in the feeder, and in turn increase the voltage in the nodes. It is thus interesting to study how this affects the feasibility. The last aspect, the loads, was chosen to be varied in order to ensure that the controller preformed as expected when the net power of the node was lower than that produced by the PV. This would mean that a lower net power, entailing a lower nodal voltage, would require less curtailment from the controller.

3.4.1 Controller Parameters

The first aspect of the system to be studied was the PI controller itself. By varying the control parameters, the test system remained constant, but made it possible to find intervals in which the controller would be stable. As with the base case, this was first tested with production in just one node, and later in two.

Looking back at eq. 2.17, the parameters which were varied was K, the proportional gain of the controller, and T_i, the integrating time constant. In order to find a suitable interval for these values, the simulations were first run by varying each parameter in the base case one by one. By doing it this way, it would make it quite simple to find an interval for each parameter where the performance of the controller could be deemed feasible. On one end of this interval, the controller would be too fast to be able to maintain stability. On the other end of this interval it would be too slow to be considered feasible to use in the system.

3.4.2 Power Lines

Next the power lines in the test system were changed. Looking back at equations 2.11 and 2.12, the voltage sensitivity is dependent on the impedance of the lines in the system. In order to study how this affected the system, the power lines were changed in two ways. First by changing the length of the lines, by multiplying the length of each line segment with a length factor, x_{length}. This would change the distance between the MV/LV substation and the end of the feeder, as well as the distance between the nodes themselves. Increasing or decreasing the length of the lines between the nodes would in practice increase or decrease the impedance between the nodes.

Second, the resistance in the lines were changed. This was done by changing the R/X ratio in the lines. Thus the reactance, X, in the lines were multiplied with a factor between 0.7 and 11, since these are values of R/X that can be expected in a LV DN, as stated earlier in section 2.3.2.

Studying the values of R and X of the lines used in the test system, it was determined that the original value for this ratio for the main radial (UG1) was R/X = 2.2, and for the branches out to each node (UG3) was R/X = 10.5. In order to only having to vary one parameter, the main radial (UG1) was chosen to be varied, and the branches remained unchanged. Since the branch to each node is so short, only 30 m (see figure 2.5), it seemed that changing the main radial would have the most effect on the result.

3.4.3 Loads

The last aspect of the system to be varied was the loads in each node. So far there have only been production in the nodes, and by applying loads as well, this would represent e.g. a house being connected to the grid at the node, and thus using power.

The load has two parts, active (P) and reactive (Q) loads. Thus when studying how the system react to different loads, the loads were first purely active and changing in magnitude, and then (almost) purely reactive and changing in magnitude. In order to change the amount of active and reactive power in the loads, the power factor ($cos\varphi$) had to be changed. $cos\varphi = 1$ would correspond to a purely active load, and $cos\varphi = 0$ to a purely reactive load. However, due to how the ANM algorithm was implemented in the Python script, it is not possible to have $cos\varphi = 0$, and thus, in order to have a load that is as close to purely reactive as possible, the power factor was set to $cos\varphi = 0.01$ when varying Q.

When varying the loads, the objective was not to find a limit where the system was no longer stable. Instead it was mainly to ensure that the controller would still function when loads, both active and reactive, were put in place. Thus the analysis of the system when varying the loads were not as rigorous as in previous cases.

Chapter 4

Results and analysis

In the previous chapter, it was established how the simulations in PowerFactory were carried out. In this chapter, the data resulting from each simulation will be presented, along with an interpretation of the obtained data.

4.1 Base case

In figure 4.1 and 4.2, the step responses resulting from the base case simulations are displayed, and key figures from the step responses are presented in table 4.1. Figure 4.1 show the step response when using one PV unit, connected in R18. Thus the voltage and power output in this node is displayed, as well as the voltage in node R1, where the transformer is connected. Figure 4.2 instead show the step response when having PV connected in both R18 and R17. Thus the voltage and power output in R17 is displayed, in addition to the previous nodes.

In figure 4.1, where only one PV unit is connected, the voltage in R18 reach a value of 1.08 p.u., which is still within the limits Ei has declared. After about 50 s the controller has managed to push down the voltage in the node to 1.05 p.u., meaning that, when using one PV in the base case, the controller fulfills the feasibility requirements that were stated in section 3.2.

In figure 4.2 the voltage in both R17 and R18 reaches a value of around 1.12 p.u. when the PV is first activated, with a slightly higher voltage in R18. These values are above that which Ei deems should be resolved in a reasonable manner, but not above any limits which are not allowed (see table 2.1). After about 40 s however, the controller has already managed to push the voltage back down to 1.05 p.u.. From this we can declare that in the base case, with two PV units, the controller fulfills the feasibility requirements.

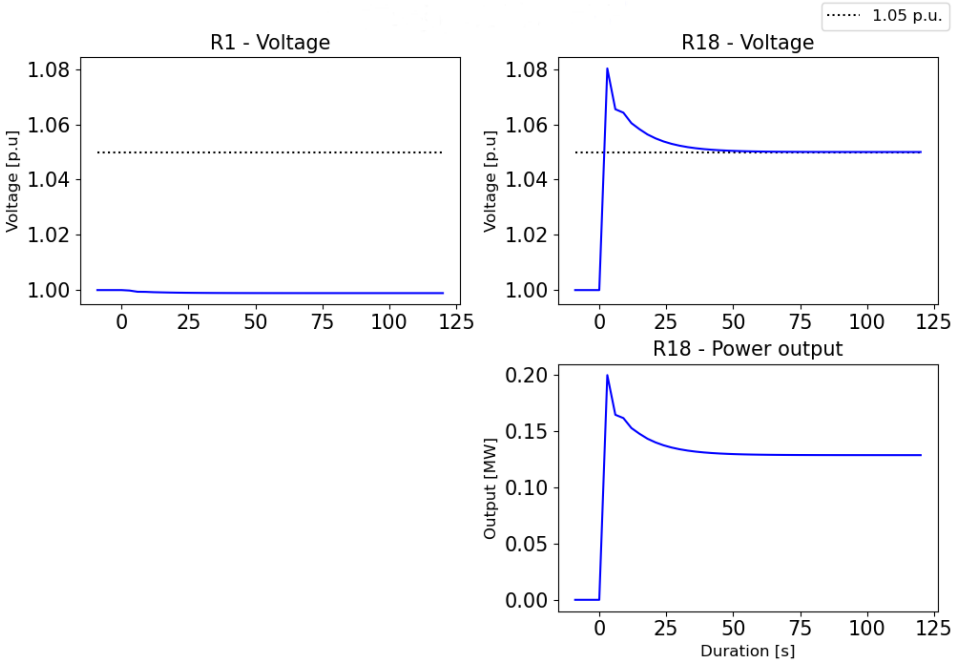

Figure 4.1: Step response resulting from base case when having one PV unit installed in the system. Key figures from the result are presented in table 4.1.

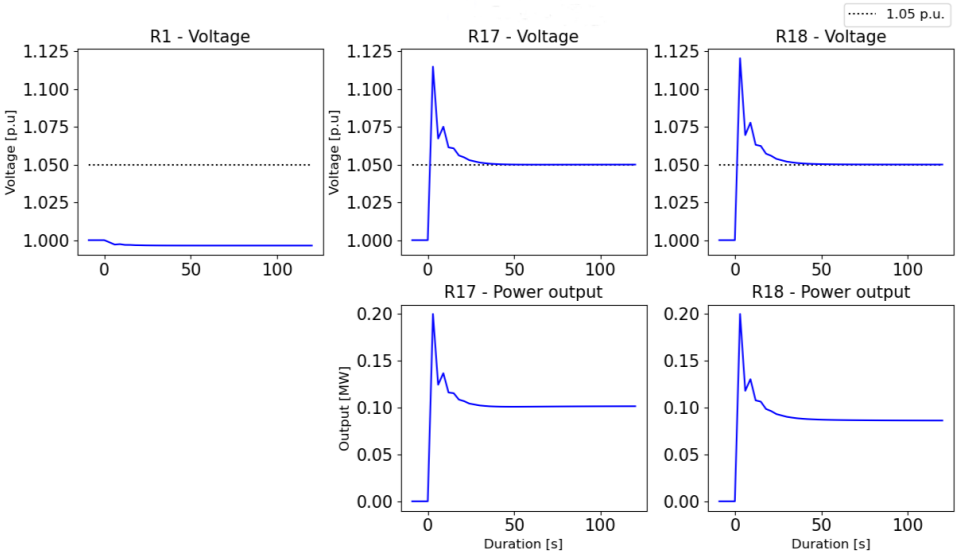

Figure 4.2: Step response resulting from base case when having two PV units installed in the system. Key figures from the result are presented in table 4.1.

Table 4.1: Key figures of the results of the base case, derived from the step responses in figures 4.1 and 4.2. V_{max} is the maximum voltage achieved in a node, T_{stab} is the time it take before the voltage has stabilised at 1.05 p.u., P_{stab} is the power output from the node after the voltage has stabilised.

Case	$V_{max,R17}$ [p.u.]	$V_{max,R18}$ [p.u.]	T_{stab} [s]	$P_{stab,R17}$ [MW]	$P_{stab,R18}$ [MW]
One PV	N/A	1.08	50	N/A	0.13
Two PV	1.12	1.12	40	0.10	0.08

Something else that can be seen in both of these cases, is that despite a significant increase in voltage at the end of the feeder, the voltage in R1 remains relatively unchanged. Thus, when studying the rest of the cases, the graph depicting the voltage in R1 will be omitted.

4.2 Varying System Parameters

In this section, the results from each test system is presented and analysed.

4.2.1 Controller parameters

In figure 4.3 the results from the simulations using one PV unit while varying the controller parameters are shown. Figure 4.3a depict the results when varying the gain, K, and figure 4.3b when varying the integrating time constant, T_i. The simulations were performed over five iterations per parameter, and the values of the active parameter for each iteration are displayed in table 4.2. Key figures from the simulations are displayed in table 4.3.

Table 4.2: Values used for K and T_i when having one PV unit installed in the system. Note that the value in **bold** is the value used in the base case.

K	0.1	0.2	**0.5**	1	1.4
T_i	0.36	0.45	**2.25**	4.5	11.25

Figure 4.3a show that the controller reach instability when $K \geq 1.4$ and in figure 4.3b when $T_i \leq 0.36$. However, this does not mean that for $K < 1.4$ or $T_i > 0.46$ the controller would always be feasible. For $K = 1$ there are some smaller oscillations, and while they are dampened fairly quickly, after 30 s the amplitude are still large enough to not fulfill the feasibility requirements. For $K = 0.2$ and $K = 0.1$ the controller is very slow. For $K = 0.2$ it takes the controller about 100 s to get the voltage back down to 1.05 p.u., and for $K = 0.1$, it is not able to push the voltage down to 1.05 p.u. within the 120 s of the simulation. Both of these controllers are thus too slow to fulfill the feasibility requirements.

For $T_i = 0.45$ the controller is so fast that oscillations occur, and while these decrease in amplitude, they do not die down completely over the 120 s simulation. Due to these lasting oscillations, the controller does not fulfill the feasibility requirements. For $T_i = 4.5$ the controller is slower than the base case, but manage to get the voltage down to 1.05 p.u. after about 90 s. While this is rather slow, it is right on the limit set for feasibility. Thus, this controller does fulfill the feasibility requirements. For $T_i = 11.25$ the controller is very slow, and is not able to push the voltage down to 1.05 p.u. within the 120 s of the simulation. Thus, the controller does not fulfill the feasibility requirements.

Table 4.3: Key figures of the results when varying K and T_i and having one PV unit installed, derived from the step responses in figures 4.3a and 4.3b. V_{max} is the maximum voltage achieved in a node, T_{stab} is the time it take before the voltage has stabilised at 1.05 p.u., $T_{osc,stab}$ is the time it takes for the amplitude of the oscillations to be reduced by 90%, P_{stab} is the power output from the node after the voltage has stabilised.

Case	Stable?	$V_{max,R18}$ [p.u.]	T_{stab} [s]	$T_{osc,stab}$ [s]	$P_{stab,R18}$ [MW]
K = 0.1	Yes	1.08	>120	N/A	N/A
K = 0.2	Yes	1.08	100	N/A	0.13
K = 0.5	Yes	1.08	50	N/A	0.13
K = 1	Yes	1.08	40	>30	0.13
K = 1.4	No	1.08	N/A	N/A	N/A
T_i = 0.36	No	1.08	N/A	N/A	N/A
T_i = 0.45	Yes	1.08	>120	>30	N/A
T_i = 2.25	Yes	1.08	50	N/A	0.13
T_i = 4.5	Yes	1.08	90	N/A	0.13
T_i = 11.25	Yes	1.08	>120	N/A	N/A

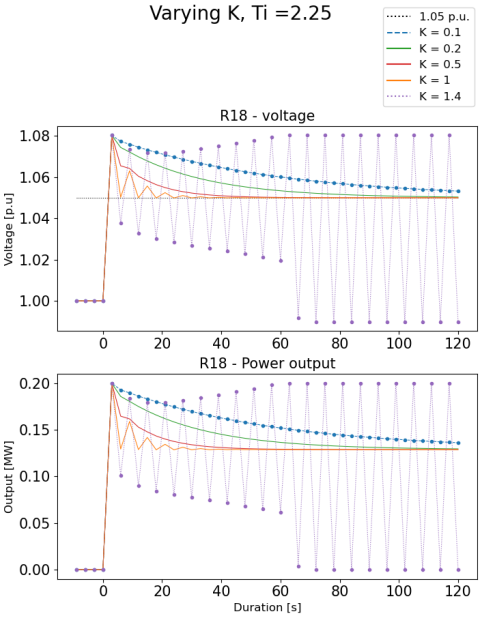

(a) Step responses when varying K, when having one PV unit installed.

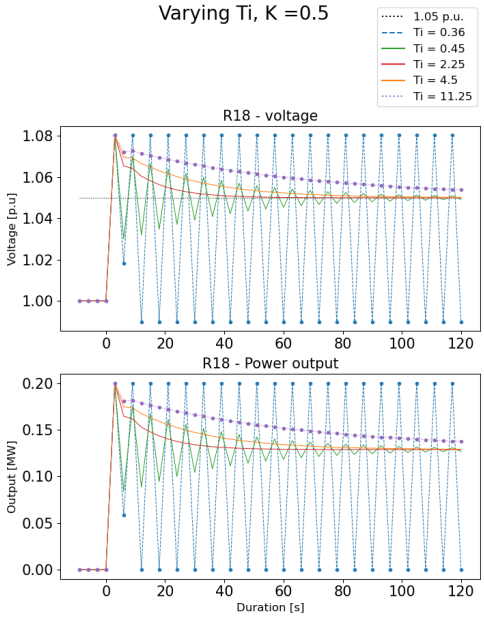

(b) Step responses when varying T_i, when having one PV unit installed.

Figure 4.3: Step responses resulting from varying PI parameters, when having one PV unit installed in the system. Key figures from the results are presented in table 4.3.

In figure 4.4 and 4.5, the results from the simulations using two PV units while varying the controller parameters are shown. Figure 4.4 depict the results when varying the gain,

K, and figure 4.5 when varying the integrating time constant, T_i. The simulations were performed over five iterations per parameter, and the values of the active parameter for each iteration are displayed in table 4.4. Key figures from the simulations are displayed in table 4.5.

Table 4.4: Values used for K and T_i when having two PV units installed in the system. Note that the value in **bold** is the value used in the base case.

K	0.1	0.2	**0.5**	0.8	1
T_i	0.72	1.125	**2.25**	4.5	11.25

Figure 4.4 show that the controller reach instability when $K \geq 1$ and in figure 4.5 when $T_i \leq 0.72$. Comparing this to the results from using one PV, the values that previously resulted in a stable system, now would make the system unstable. This would mean that more PV units in the same feeder would lower the limit for when the system become unstable. However, it should also be noted that when having two controllers working together, it makes them faster. As noted in the base case, despite the voltage reaching a higher value, the controllers manages to get it back to 1.05 p.u. in 40 s, as opposed to 50 s when only having one PV unit installed.

Furthermore, in figure 4.4, it is noted that when $K = 0.2$, the controller get the voltage down to 1.05 p.u. in 85 s, as opposed to 100 s from before, and could thus manage to fulfill the feasibility requirements. When $K = 0.1$, the voltage still never quite reach 1.05 p.u. in 120 s, but the difference is much less than for one controller, with only about 0.002 p.u. to go. Despite this, the controller does not fulfill the feasibility requirements. When $K = 0.8$, the controllers have not yet reached instability. However, oscillations do occur that remain for a significant amount of time. Thus, this controller does not fulfill the feasibility requirements.

Looking instead at figure 4.5, when $T_i = 4.5$, the voltage is brought down in about 75 s, as opposed to 90 s when having one controller. This is considered well within the feasibility requirements. For $T_i = 11.25$, the controllers are still too slow to bring the voltage down to 1.05 p.u. in 120 s. Thus, the controller does not fulfill the feasibility requirements. When $T_i = 1.125$ oscillations occur which do decrease in amplitude. However, there are still oscillations remaining after 30 s, thus deeming the controller to not fulfill the feasibility requirements.

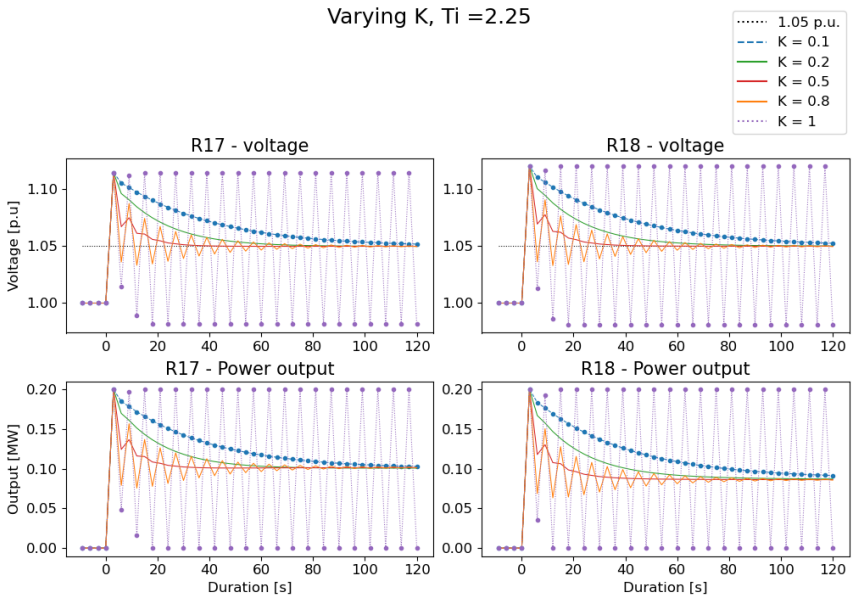

Figure 4.4: Step responses resulting from varying K, when having two PV units installed in the system. Key figures from the results are presented in table 4.5.

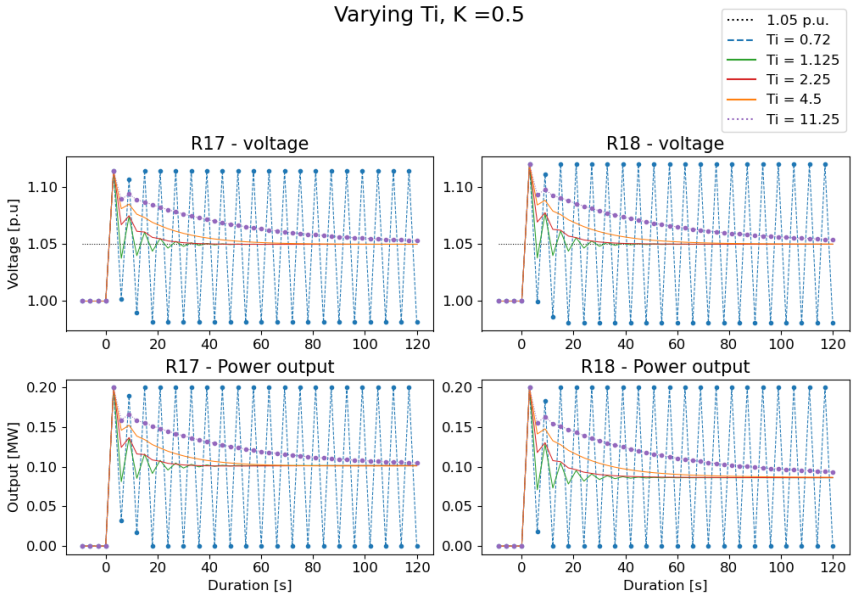

Figure 4.5: Step responses resulting from varying T_i, when having two PV units installed in the system. Key figures from the results are presented in table 4.5.

Table 4.5: Key figures of the results when varying K and T_i and having two PV units installed, derived from the step responses in figures 4.4 and 4.5. V_{max} is the maximum voltage achieved in a node, T_{stab} is the time it take before the voltage has stabilised at 1.05 p.u., $T_{osc,stab}$ is the time it takes for the amplitude of the oscillations to be reduced by 90%, P_{stab} is the power output from the node after the voltage has stabilised.

Case	Stable?	$V_{max,R17}$ [p.u.]	$V_{max,R18}$ [p.u.]	T_{stab} [s]	$T_{osc,stab}$ [s]	$P_{stab,R17}$ [MW]	$P_{stab,R18}$ [MW]
K = 0.1	Yes	1.12	1.12	>120	N/A	N/A	N/A
K = 0.2	Yes	1.12	1.12	85	N/A	0.10	0.08
K = 0.5	Yes	1.12	1.12	40	N/A	0.10	0.08
K = 0.8	Yes	1.12	1.12	110	>30	0.10	0.08
K = 1	No	1.12	1.12	N/A	N/A	N/A	N/A
$T_i = 0.72$	No	1.12	1.12	N/A	N/A	N/A	N/A
$T_i = 1.125$	Yes	1.12	1.12	45	>30	0.10	0.08
$T_i = 2.25$	Yes	1.12	1.12	40	N/A	0.10	0.08
$T_i = 4.5$	Yes	1.12	1.12	75	N/A	0.10	0.08
$T_i = 11.25$	Yes	1.12	1.12	>120	N/A	N/A	N/A

4.2.2 Power Lines

In figure 4.6, the results from varying the line parameters, when using one PV unit, are displayed. Figure 4.6a show the results when varying the resistance, R, in the lines, and figure 4.6b show when varying the length of the lines, by multiplying the original length of the line segments with a factor x_{length}. In table 4.6, the parameter values used are displayed. Key figures from the simulations are displayed in table 4.7.

Table 4.6: Values used for R/X and x_{length} when having one PV unit installed in the system. Note that the value in **bold** is the value used in the base case.

R/X	0.7	**2.2**	5.0	7.5	8.5
x_{length}	0.5	**1**	2	2.5	3

Looking at figure 4.6, it can be determined that R/X and line length does not seem to have any effect on the speed of the controller. For all iterations (that exceed 1.05 p.u.), the controller manage to get the voltage back down to 1.05 p.u. in roughly the same amount of time, but seem to vary between 40 - 50 s. However, due to the increased impedance in the feeder, the voltage in the node increase as well. This seem to have an effect on the stability of the controller, since greater values for both R and x_{length}, push the system closer to instability. The system become unstable when $R/X \geq 8.5$ or $x_{length} \geq 3$.

Figure 4.6a show that when $R/X = 0.7$, the lower resistance of the lines result in a voltage in the node that is so low, that the controller is never needed. When $R/X = 5.0$, the increased resistance does cause some oscillations, but they die down fairly quick, and after 30 s the oscillations are negligible. Thus, the controller does fulfill the feasibility requirements. However, it is worth noting that during the step in production, the voltage reach a voltage of 1.15 p.u.. According to the limits set by Ei (table 2.1), these voltages are not allowed for more than 5 s. In this case, the voltage does stay well below this limit, and

can thus still be deemed to fulfill the feasibility requirements. When $R/X = 7.5$, oscillations occur, and while these do decrease in amplitude, they still remain after 30 s. Thus, for this case, the controller cannot be deemed to fulfill the feasibility requirements. Furthermore, the voltage reach a value of 1.2 p.u.. This is still below the absolute limit of 1.35 p.u. that is set by Ei. It takes around 2 s for the voltage to drop below 1.15 p.u., and is thus still below the limit of voltage over 1.15 p.u. for no more than 5 s set by Ei.

Figure 4.6b show that when halving the line length, $x_{length} = 0.5$, the voltage in R18, again, does not reach 1.05 p.u., and the controller is thus never needed. When the length is doubled, $x_{length} = 2$, oscillations occur, but die down quickly, and does not remain after 30 s. Thus, for this case the controller fulfill the feasibility requirements. In this case the voltage reach a value of 1.15 p.u., but is immediately pushed down by the controller and is thus below the limits set by Ei. When $x_{length} = 2.5$ oscillations occur. These oscillations manage to die down eventually, but it takes around 100 s for them to do so. Because of these lasting oscillations, the controller in this case does not fulfill the feasibility requirements. Furthermore, the voltage reach a max. value of 1.18 p.u., but only stays above 1.15 p.u. for 1 s, and thus do not exceed any limits set by Ei.

Table 4.7: Key figures of the results when varying R/X and x_{length} and having one PV unit installed, derived from the step responses in figure 4.6. V_{max} is the maximum voltage achieved in a node, T_{stab} is the time it take before the voltage has stabilised at 1.05 p.u., $T_{osc,stab}$ is the time it takes for the amplitude of the oscillations to be reduced by 90%, P_{stab} is the power output from the node after the voltage has stabilised.

Case	Stable?	$V_{max,R18}$ [p.u.]	T_{stab} [s]	$T_{osc,stab}$ [s]	$P_{stab,R18}$ [MW]
$R/X = 0.7$	Yes	1.04	N/A	N/A	0.20
$R/X = 2.2$	Yes	1.08	50	N/A	0.13
$R/X = 5.0$	Yes	1.15	40	<30	0.07
$R/X = 7.5$	Yes	1.20	>120	>30	N/A
$R/X = 8.5$	No	1.22	N/A	N/A	N/A
$x_{length} = 0.5$	Yes	1.04	N/A	N/A	0.20
$x_{length} = 1$	Yes	1.08	50	N/A	0.13
$x_{length} = 2$	Yes	1.12	40	<30	0.07
$x_{length} = 2.5$	Yes	1.12	100	>30	0.06
$x_{length} = 3$	No	1.21	N/A	N/A	N/A

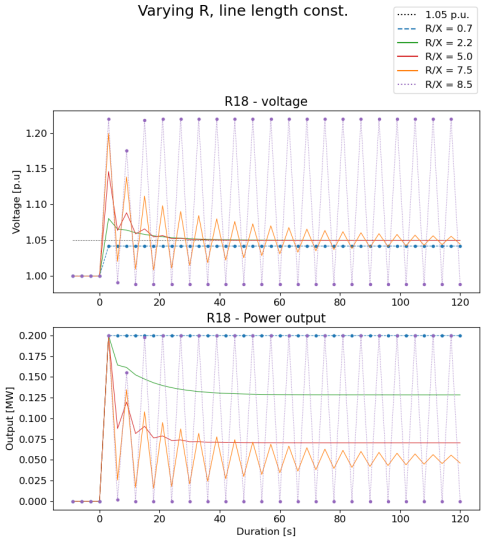

(a) Step responses resulting from varying the R/X ratio, when having one PV unit installed in the system.

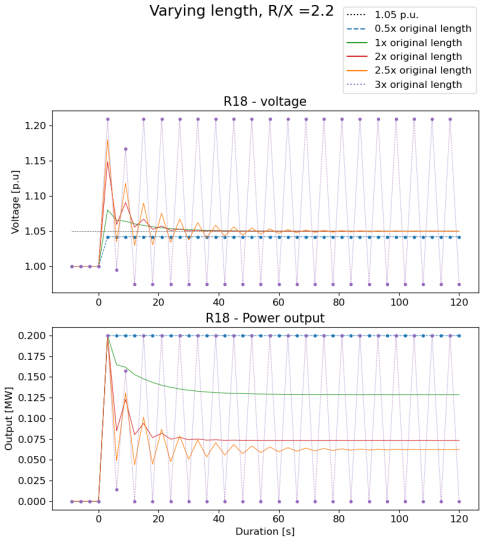

(b) Step responses resulting from varying line lengths, when having one PV unit installed in the system.

Figure 4.6: Step responses resulting from varying the properties of the power lines, when having one PV unit installed in the system. Key figures from the results are presented in table 4.7.

In figure 4.7 and 4.8, the results from varying the line parameters, when using two PV units, are displayed. Figure 4.7 show the results when varying the resistance, R, in the lines, and figure 4.8 show when varying the length of the lines. In table 4.8, the parameter values used are displayed. Key figures from the simulations are displayed in table 4.9.

Table 4.8: Values used for R/X and x_{length} when having two PV units installed in the system. Note that the value in **bold** is the value used in the base case.

R/X	0.7	1.5	**2.2**	3.25	5.0
x_{length}	0.25	0.5	**1**	1.5	2

Figure 4.7 show that the system become unstable when $R/X \geq 5.0$. For $R/X = 0.7$, the voltage in R17 still stay below 1.05 p.u., and in R18 it only slightly exceed that. Thus only the controller in R18 is needed to push down the voltage, and both controllers fulfill the feasibility requirements. When $R/X = 1.5$ the voltage in both nodes stay below any limits set by Ei, and the controllers can get the voltage down within 90 s. For this case the controllers fulfill the feasibility requirements. When $R/X = 3.25$, the voltage in R17 reach a maximum of 1.15 p.u., and in R18 it reach 1.16 p.u.. However, the voltage in R18 stays exceed 1.15 p.u. for only about 0.5 s, and thus does not exceed any limits. Furthermore, in this case, oscillations occur when the controllers decrease the voltage. When measuring these oscillations, after 30 s they have decreased with almost exactly 90%. So while it is just on the limit, the controllers do fulfill the feasibility requirements.

Figure 4.8 show that the system become unstable when $x_{length} \geq 2$. For $x_{length} = 0.25$, the voltage in both nodes remain below 1.05 p.u., and no controller is thus needed. For

$x_{length} = 0.5$ the voltage in both nodes exceed 1.05 p.u., but only reach 1.06 p.u., and is quickly brought down to 1.05 p.u. again. In this case the controllers are thus deemed to fulfill the feasibility requirements. When $x_{length} = 1.5$ the voltage in R17 reach a maximum of 1.16 p.u., and is above 1.15 p.u. for 0.5 s. In R18 the voltage reach a maximum of 1.17 p.u., and is above 1.15 p.u. for 1 s. The voltage in both nodes are thus well below any limits set by Ei. However, there are oscillations that occur that still remain after 30 s. Thus, the controllers do not fulfill the feasibility requirements.

Table 4.9: Key figures of the results when varying R/X and x_{length} and having two PV units installed, derived from the step responses in figures 4.7 and 4.8. V_{max} is the maximum voltage achieved in a node, T_{stab} is the time it take before the voltage has stabilised at 1.05 p.u., $T_{osc,stab}$ is the time it takes for the amplitude of the oscillations to be reduced by 90%, P_{stab} is the power output from the node after the voltage has stabilised.

Case	Stable?	$V_{max,R17}$ [p.u.]	$V_{max,R18}$ [p.u.]	T_{stab} [s]	$T_{osc,stab}$ [s]	$P_{stab,R17}$ [MW]	$P_{stab,R18}$ [MW]
$R/X = 0.7$	Yes	1.05	1.05	N/A	N/A	0.20	0.20
$R/X = 1.5$	Yes	1.08	1.09	40	N/A	0.13	0.11
$R/X = 2.2$	Yes	1.12	1.12	40	N/A	0.10	0.08
$R/X = 3.25$	Yes	1.15	1.16	40	>30	0.07	0.05
$R/X = 5.0$	No	1.12	1.12	N/A	N/A	N/A	N/A
$x_{length} = 0.25$	Yes	1.03	1.03	N/A	N/A	0.2	0.2
$x_{length} = 0.5$	Yes	1.06	1.06	40	N/A	0.17	0.15
$x_{length} = 1$	Yes	1.12	1.12	40	N/A	0.10	0.08
$x_{length} = 1.5$	Yes	1.16	1.17	40	>30	0.07	0.06
$x_{length} = 2$	No	1.21	1.22	N/A	N/A	N/A	N/A

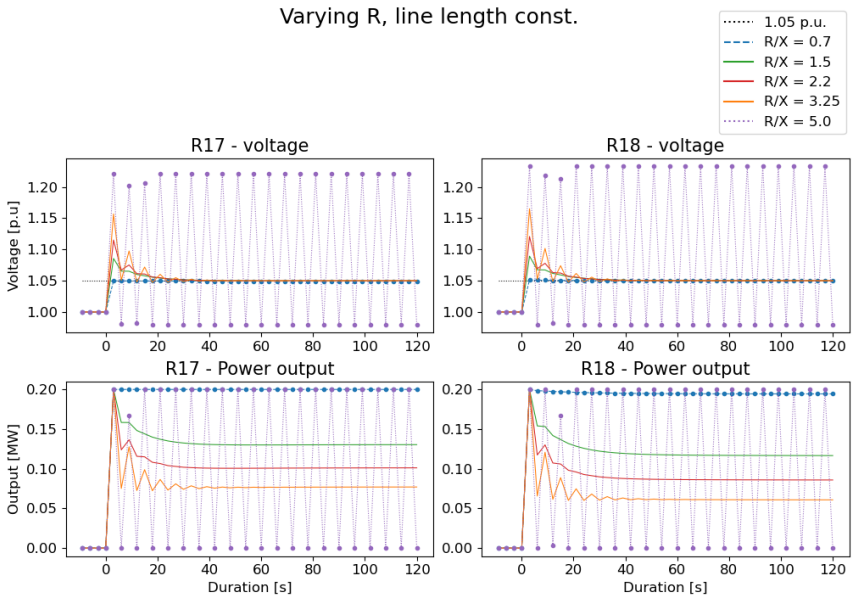

Figure 4.7: Step responses resulting from varying the R/X ratio, when having two PV units installed in the system. Key figures from the results are presented in table 4.9.

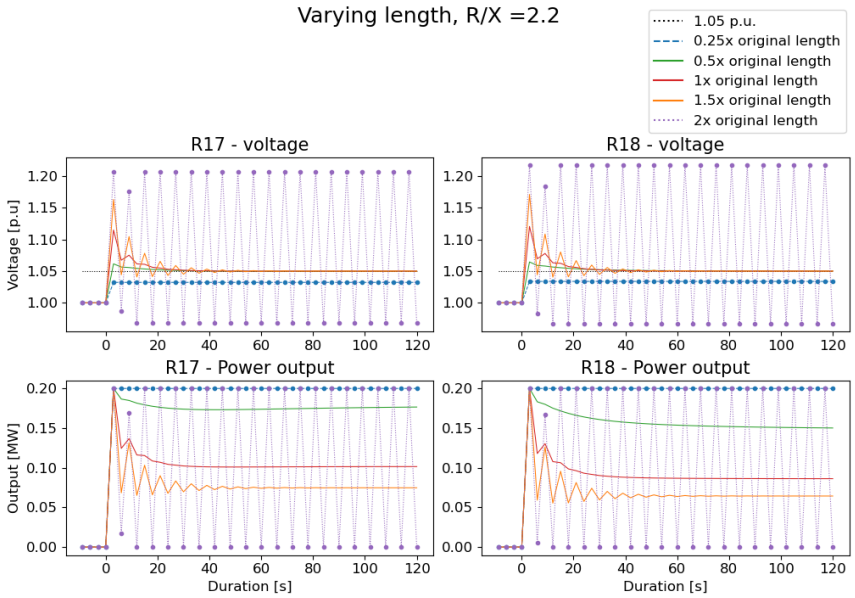

Figure 4.8: Step responses resulting from varying line lengths, when having two PV units installed in the system. Key figures from the results are presented in table 4.9.

4.2.3 Loads

In figure 4.9, the results from varying the loads, when using one PV unit. In 4.9a, the active load, P, is being varied, and in 4.9b, the reactive load, Q, is being varied. Key figures from the simulations are displayed in table 4.11. In table 4.10, the values of the apparent power, S, of the load used are displayed. Worth noting is both when P and Q, the actual parameter being varied is S, and for the two different simulations, different values of the power factor, $cos\varphi$, is used. When varying P $cos\varphi = 1.0$, in order to achieve a purely active load, and when varying Q $cos\varphi = 0.01$, in order to achieve a close to purely reactive load.

Table 4.10: Values used for the apparent power of the loads when having one PV unit installed in the system. Note that the value in **bold** is the value used in the base case.

S [kVA]	**0**	25	50	75	100

Figure 4.9 show that, with increasing load, the voltage in the node decrease. Figure 4.9a show that when $S \geq 75$ kVA, the voltage no longer exceed 1.05 p.u., and thus the controller is no longer needed. Figure 4.9b show that, when the load is reactive, even for $S = 100$ kVA, the voltage exceed 1.05 p.u.. It is worth noting that the power output from the PV unit is purely active. This means that when the load is purely active as well, it will decrease the net active power output from the node, and thus significantly reduce the voltage in the node, as would be expected from equations 2.11 and 2.12.

Table 4.11: Key figures of the results when varying active and reactive loads and having one PV unit installed, derived from the step responses in figure 4.9. V_{max} is the maximum voltage achieved in a node, T_{stab} is the time it take before the voltage has stabilised at 1.05 p.u., $T_{osc,stab}$ is the time it takes for the amplitude of the oscillations to be reduced by 90%, P_{stab} is the power output from the node after the voltage has stabilised.

Case	Stable?	$V_{max,R18}$ [p.u.]	T_{stab} [s]	$T_{osc,stab}$ [s]	$P_{stab,R18}$ [MW]
$cos\varphi = 1$					
$S = 0$ kVA	Yes	1.08	50	N/A	0.13
$S = 25$ kVA	Yes	1.07	50	N/A	0.15
$S = 50$ kVA	Yes	1.06	50	N/A	0.18
$S = 75$ kVA	Yes	1.05	N/A	N/A	0.20
$S = 100$ kVA	Yes	1.035	N/A	N/A	0.20
$cos\varphi = 0.01$					
$S = 0$ kVA	Yes	1.08	50	N/A	0.13
$S = 25$ kVA	Yes	1.075	50	N/A	0.14
$S = 50$ kVA	Yes	1.07	50	N/A	0.16
$S = 75$ kVA	Yes	1.06	50	N/A	0.175
$S = 100$ kVA	Yes	1.055	50	N/A	0.19

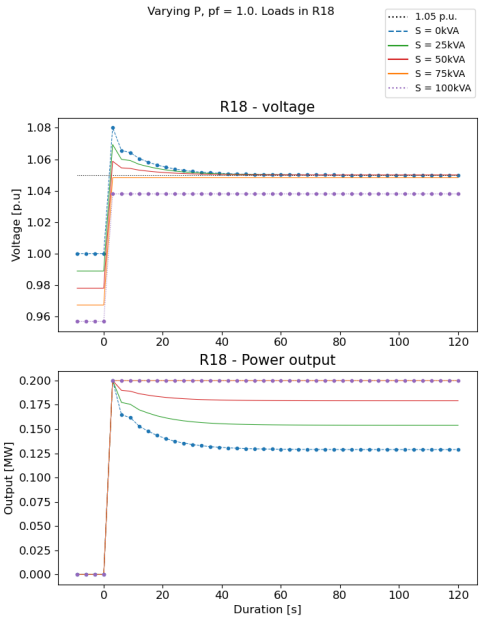

(a) Step responses resulting from varying active loads, when having one PV unit installed in the system.

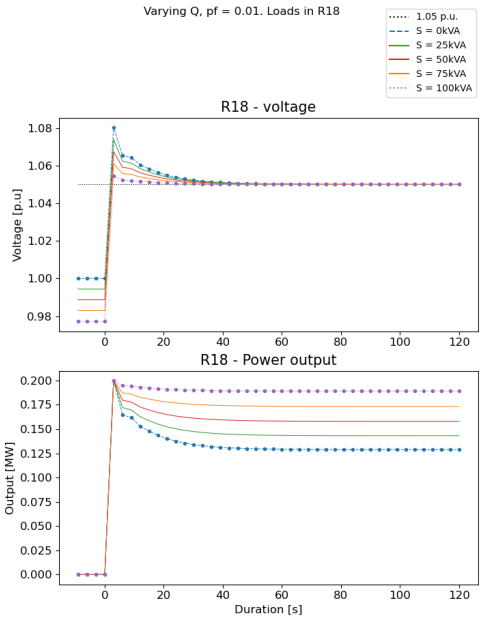

(b) Step responses resulting from varying reactive loads, when having one PV unit installed in the system.

Figure 4.9: Step responses resulting from varying the loads connected to the node, when having one PV unit installed in the system. Key figures from the results are presented in table 4.11.

In figure 4.10 and 4.11, the results from varying the loads, when using two PV units. In 4.10, the active load, P, is being varied, and in 4.11, the reactive load, Q, is being varied. Key figures from the simulations are displayed in table 4.13. In table 4.12, the values of the apparent power, S, of the load used are displayed. Again, the apparent power of the loads remain the same both when varying P and Q, but $cos\varphi = 1.0$ when using an active load, and $cos\varphi = 0.01$ when using a reactive load. Furthermore, the loads are of equal size in both nodes, and the S presented in table 4.12 is the size of the load in each node.

Table 4.12: Values used for the apparent power of the loads when having two PV units installed in the system. Note that the value in **bold** is the value used in the base case.

S [kVA]	**0**	50	75	100	150

Figure 4.10 show that when $S = 100$ kVA, the voltage in both nodes only slightly exceed 1.05 p.u., and any load greater than that would result in the voltage never exceeding this limit. When comparing these results to that when only using one PV unit, it can be seen that the loads need to be greater when using two PV in order to achieve the same effect on the voltage. When using two PV units, due to the increase in power output, the voltage increase even when no load is connected. It should also be remembered that the power in R17 affect the voltage in R18 and vice versa. This explains why a greater load in each node is needed to see the same effect as when only using one PV unit.

Figure 4.11 show that when $S = 150$ kVA, the voltage in both nodes never exceed 1.05 p.u., and thus the controllers are no longer needed. Just as when only one PV unit was active, the reactive load has less of an effect on the voltage than an active load. Furthermore, just as with the active loads, when using two PV units, a greater load is required to have the same effect on the voltage compared to only one PV unit.

Table 4.13: Key figures of the results when varying active and reactive loads and having two PV units installed, derived from the step responses in figures 4.10 and 4.11. V_{max} is the maximum voltage achieved in a node, T_{stab} is the time it take before the voltage has stabilised at 1.05 p.u., $T_{osc,stab}$ is the time it takes for the amplitude of the oscillations to be reduced by 90%, P_{stab} is the power output from the node after the voltage has stabilised.

Case	Stable?	$V_{max,R17}$ [p.u.]	$V_{max,R18}$ [p.u.]	T_{stab} [s]	$T_{osc,stab}$ [s]	$P_{stab,R17}$ [MW]	$P_{stab,R18}$ [MW]
$cos\varphi = 1$							
$S = 0$ kVA	Yes	1.12	1.12	40	N/A	0.10	0.08
$S = 50$ kVA	Yes	1.08	1.08	40	N/A	0.15	0.14
$S = 75$ kVA	Yes	1.065	1.065	40	N/A	0.17	0.16
$S = 100$ kVA	Yes	1.055	1.055	20	N/A	0.20	0.19
$S = 150$ kVA	Yes	1.02	1.02	N/A	N/A	0.20	0.20
$cos\varphi = 0.01$							
$S = 0$ kVA	Yes	1.12	1.12	40	N/A	0.10	0.08
$S = 50$ kVA	Yes	1.09	1.09	40	N/A	0.14	0.12
$S = 75$ kVA	Yes	1.075	1.075	40	N/A	0.16	0.14
$S = 100$ kVA	Yes	1.06	1.06	40	N/A	0.18	0.16
$S = 150$ kVA	Yes	1.04	1.04	N/A	N/A	0.20	0.20

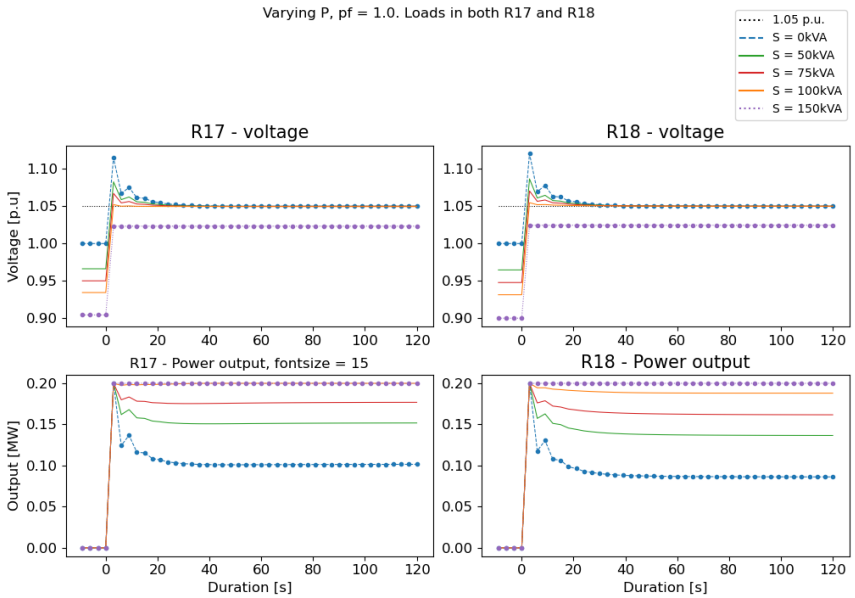

Figure 4.10: Step responses resulting from varying active loads in the nodes, when having two PV units installed in the system. Key figures from the results are presented in table 4.13.

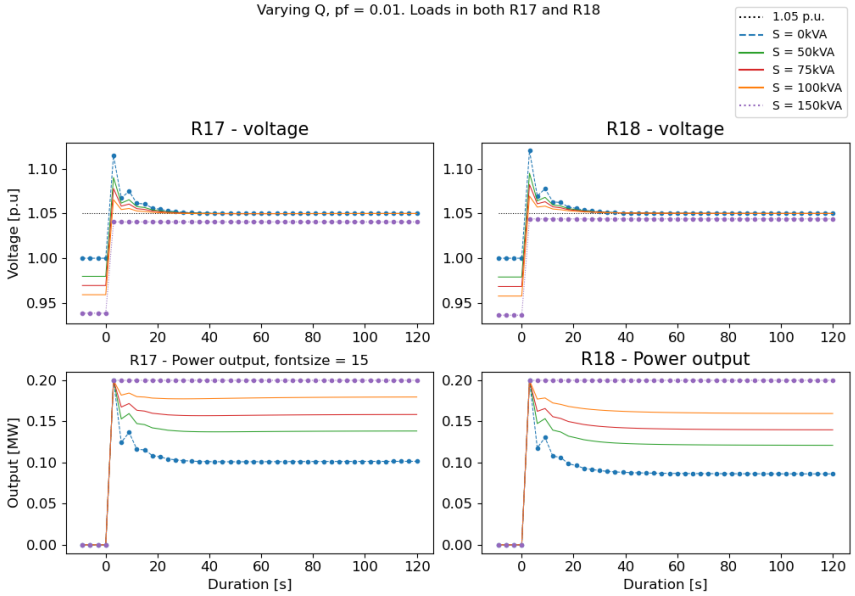

Figure 4.11: Step responses resulting from varying reactive loads in the nodes, when having two PV units installed in the system. Key figures from the results are presented in table 4.13.

4.3 Summary

By varying the different parameters of the system and testing the controller on each case, there seem to be a range of values for each parameter where the controller is feasible. There is also a range where the system is stable but the controller do not fulfill the feasibility criteria. For all values of loads on the nodes, the controller is feasible, due to when connecting a load to the node, it will only affect the net power output from the node. Thus the controller itself is not affected by the load, but simply experience a lesser overvoltage that need to be resolved.

When varying the PI parameters and the properties of the power lines however, there seem to be intervals where the system is stable and a narrower interval where it is also feasible. In tables 4.14 and 4.15 the values tested are summarised, along whether the system for each case is unstable, stable, or feasible.

Table 4.14: Summary of the PI parameters tested, and the characteristics of the system for each case. For all cases stated, the line parameters are $R/X = 2.2$ and $x_{length} = 1$. When varying K, $T_i = 2.25$, and when varying T_i, $K = 0.5$.

One PV		Two PV	
$K = 0.1$	Stable	$K = 0.1$	Stable
$K = 0.2$	Stable	$K = 0.2$	Feasible
$K = 0.5$	Feasible	$K = 0.5$	Feasible
$K = 1$	Stable	$K = 0.8$	Stable
$K = 1.4$	Unstable	$K = 1$	Unstable
$T_i = 0.36$	Unstable	$T_i = 0.72$	Unstable
$T_i = 0.45$	Stable	$T_i = 1.125$	Stable
$T_i = 2.25$	Feasible	$T_i = 2.25$	Feasible
$T_i = 4.5$	Feasible	$T_i = 4.5$	Feasible
$T_i = 11.25$	Stable	$T_i = 11.25$	Stable

Table 4.15: Summary of the power line parameters tested, and the characteristics of the system for each case. For all cases stated, the PI parameters are $K = 0.5$ and $T_i = 2.25$. When varying R/X, $x_{length} = 1$, and when varying x_{length}, $R/X = 2.2$.

One PV		Two PV	
$R/X = 0.7$	Feasible	$R/X = 0.7$	Feasible
$R/X = 2.2$	Feasible	$R/X = 1.5$	Feasible
$R/X = 5.0$	Feasible	$R/X = 2.2$	Feasible
$R/X = 7.5$	Stable	$R/X = 3.25$	Stable
$R/X = 8.5$	Unstable	$R/X = 5.0$	Unstable
$x_{length} = 0.5$	Feasible	$x_{length} = 0.25$	Feasible
$x_{length} = 1$	Feasible	$x_{length} = 0.5$	Feasible
$x_{length} = 2$	Feasible	$x_{length} = 1$	Feasible
$x_{length} = 2.5$	Stable	$x_{length} = 1.5$	Stable
$x_{length} = 3$	Unstable	$x_{length} = 2$	Unstable

Chapter 5

Discussion

In the previous chapter, the results from the simulations were presented. In this final chapter, these results are used in a discussion around the problem statements of this thesis. The discussion is then used to draw conclusions from the work, as well as to contemplate what future research might be needed in order to achieve a greater understanding of the problem.

5.1 Relationship Between System Parameters and Feasibility

The main objective in this thesis has been to study the stability of the ANM controller algorithm in different test systems. In section 4.2 it could be determined that certain system parameters did have a significant effect on the stability of the controller, while others had virtually no effect.

In figures 4.9 - 4.11 it shows that the load in the node do not seem to have any effect on the controller. The only effect the load had on the node was lowering the net power leaving the node. This in turn lowered the initial voltage in the node when the PV was activated, and thus lowering the need for the controller.

When varying the parameters of the power lines however, this heavily impacted the stability of the controller. In figures 4.6 - 4.8 it shows that larger resistance, R, and longer power lines will push the controller closer to instability. It should also be noted that the longer power lines will in turn also result in higher resistance in the entire system.

With this, and the results from the controller parameters being varied, a conclusion can be drawn that there seem to be a relation between the resistance in the system, the controller parameters, the number of controllers in the system, and the stability of the entire system. Looking back at section 2.3.5, when introducing the PI controller to a DN, the dynamics of the controller along with the properties of the DN could both be explained as the closed loop gain. Thus it would seem that a larger loop gain would bring the system closer to instability, and would make the performance less feasible. From this, and the relations discussed, it would seem that the loop gain and the properties of the system would be related according to:

$$Loop\,Gain \propto R \cdot \frac{K}{T_i} \cdot N_{PV} \tag{5.1}$$

This relation could thus be used when fitting controllers to a system. If the relation in equation 5.1 could be numerically determined, this, along with the physical properties of the DN, could be used as a rule of thumb when implementing the ANM algorithm. What is worth noting is that there are parameters in this relation that would be more or less possible to affect. The resistance of the feeder is difficult to change. This would require reconfiguration or swapping the cables of the DN. Just as was discussed with reinforcement of a network, this would cost a lot of money, and take a long time. The number of PV units installed in a DN is somewhat possible to affect. While it is possible to install new PV, or determine an upper limit to the amount installed in a DN, it is unlikely that any PV already installed into a system would be removed. One could argue that if a unit is old or faulty, and it would be to expensive to replace or repair, it would instead just be removed. However, this feels like an unlikely scenario, and in general, if a unit is installed, it is there to stay. What is easy to affect however, is the controller parameters. When the system is implemented into a system, these have to be decided upon as the controllers are tuned. The idea of this rule of thumb is that, depending of the properties of the system at large, this relationship can be used in order to tune the controllers. Hopefully it could also be used to determine the performance of the controller in a given system, and it could be tuned to achieve different behaviors depending on what is desired.

5.2 Number of Controllers

Already in the base case there was a difference in the results between when there was only one PV unit, and when there was two units installed. The first obvious difference was the increased voltage in the nodes. Having two 200 kW PV units installed means there is twice the amount of power being injected to the DN. Since an increase in voltage in one node will affect the entire feeder, the power injected at each node will not only affect the voltage in that node, but in all nodes.

Another thing that can be noted in the base case is the speed of the controllers increasing when using two. When using one controller, the voltage in node R18 was reduced down to 1.05 p.u. in 50 s, and while using two controllers the voltage was brought down to 1.05 p.u. in 40 s. This is despite the increase in the initial voltage. This can be explained in the same way as the voltage increase was explained. When there are two controllers in the feeder, despite that each controller only controls the voltage in the respective node, the controller's actions will also affect the voltage of the other nodes in the feeder. Thus, when the controller in one of the nodes manages to reduce the voltage by an amount, the decrease in power output from this node will lead to a reduction in the voltage in the other node by some amount. Thus the voltage will be reduced more than the one controller had intended, and the voltage will be brought back down in a shorter time.

However, the faster controllers could also in part be explained by the increased voltage. Since the initial voltage is higher when having two PV units, there will also be a larger error between the measured voltage and the desired voltage. A larger error will result in a more aggressive controller, and thus could decrease the time it takes for the voltage to be brought down to the desired level, by some small amount.

When varying the different parameters, there are issues that come to fruition as a result of the increased speed of the controllers. When the controller parameters are studied, it is clear that the system is more sensitive to instability when using two controllers instead of one. When using two controllers, the system will reach instability at a lower gain ($K = 1$) and a higher integrator constant ($T_i = 0.72$) than when using only one controller ($K = 1.4$

and $T_i = 0.36$). However, due to the increased speed of the controllers, they are also feasible at lower values for K and higher values for T_i than when using one controller.

Furthermore, when varying the length and resistance of the power lines, this is also affected by the increased speed when using two controllers. When using one controller, the system reached instability when $R/X = 8.5$ and $x_{length} = 3$. When using two controllers, the system reached instability when $R/X = 5.0$ and $x_{length} = 2$. This shows that the physical properties of the feeder could possibly limit the number of PV units installed.

These findings do somewhat contradict the idea of a "plug-and-play" solution. It is clear that what fits for a system with just one controller, might not be fitting when having more controllers involved. Thus, if one would want to have a plug-and-play solution, one would have to find controller parameters according to the feeder, that is still suitable when increasing the number of PV units in the system. As was seen when varying the line parameters, these controller parameters is also not a "one size fits all", but has to be determined with regard to the physical properties of the feeder. However, as stated previously, the increased speed when using more controllers, also mean that they are feasible for lower values of K or higher values for T_i. Thus, one could imagine a plug-and-play solution where the controller is too slow, when having only a few units installed, in order to assure that the controllers remain stable as more are installed. Considering a small amount of DG in a system will have a much smaller effect on the voltage in the DN, it could still be acceptable to have a slower controller.

It should however be noted that these conclusions are extrapolated from going only from one to two controllers. In order to properly confirm these findings, it should also be tested with a larger system, with a larger amount of controllers working together.

5.3 Conclusions

The ANM algorithm studied throughout this work show great potential to avoid overvoltage in a DN by local control of active power injection from a PV unit. The stability and feasible performance of the algorithm is however dependent of several properties of the entire system. As was shown in the base case, adding more units that cooperate to a feeder, increase the speed of the controllers. The faster controllers in turn are more sensitive to other aspects of the system which might turn it unstable. The overall sensitivity and feasibility of the system seemed to depend on the loop gain of the closed loop system, where an increase in loop gain made the performance of the system less likely to be feasible. Thus, the loop gain of the system seem to be proportional to the number of PV units in the system.

When varying the controllers of the system, there was a limit to both the proportional gain (K) and the integrating time constant (T_i) where the controller were no longer stable. Furthermore, there was an interval of each value where the system was considered feasible. When more PV units were active, because of the increased speed, the interval for K was shifted down, and for T_i was shifted up. Thus, the loop gain seem to be proportional to K, and inverse proportional to T_i.

When varying the power lines of the system, there was an upper limit to both the length of the cables and their resistance, R, where the system turned unstable, but there was no lower limit to where the performance was no longer feasible. Increasing the length of the power lines does in turn also increase the resistance in the system. Thus, it would seem that the loop gain is proportional to R. When increasing the number of PV units, the upper limit for both the length and the resistance of the cables was lowered.

When varying the loads connected to each node, both the active (P) and reactive (Q)

part of the loads were varied. However, the increased load in the node only seemed to decrease the net amount of power out from the node, and thus lowering the nodal voltage. Thus the load did not have any effect on the feasibility of the system. Worth noting however, is that Q had a lesser effect on the voltage than P, which is to be expected due to the high R/X ratio of the DN, and how the voltage sensitivity for active and reactive power is related to the impedance of the system.

To summarise, the main conclusion of this thesis is that whether the performance of a system is feasible or not is dependant of the loop gain of the entire system. This loop gain is related to different properties of the system, according to:

$$Loop\,Gain \propto R \cdot \frac{K}{T_i} \cdot N_{PV}$$

5.4 Further Research

Throughout the research for this thesis, we managed to encounter several results which could (and should) be studied closer. For every question mark that was straightened, another four seemed to pop up, and it was tempting to run down every single side track. But due to time constraints, eventually lines had to be drawn, and side tracks had to be blocked off. But here I will present a few of these side tracks, which ought to be investigated in the future.

In this thesis, the performance of the controller was only analysed when avoiding over-voltage. The control method presented does have the ability to avoid congestion as well. If this were to be studied, it would be interesting to see how the performance of the system differs when controlling current or voltage. Would the same parameters have an impact on the performance? Would the stability limits change at all?

In the early stages of this research, there was an idea of using Monte Carlo methods in order to generate new test systems, with varying parameters, and see how the system would respond. Again, due to time constraints, this was never implemented. However, it would be interesting to study how the performance would change if more than one parameter was varied at one time. For instance, how would changing the gain of the controller affect how long the power lines could be before the system becomes unstable?

The test systems used also never had more than two PV units active at once. This was also an aspect of the network that had originally been planned to vary, but had to be cut out. It would be interesting to see how the controllers change when the number of units installed increase. Is the speed of the controllers proportional to the number of units? Does it ever pan out? Is there a maximum number of units which could be installed before the system is permanently unstable?

In the same line of thought, there was a relation found during this thesis, between the stability and some of the parameters studied. This relationship should definitely be studied closer. As was mentioned when discussing this relation, it could possibly be used as a rule of thumb if the method would ever be fitted to a system. But in order to achieve this, there would need to be further research performed in order to find values for this relation.

Bibliography

[1] Mats Karlström. Debatt: Trängsel hotar solcellsutbyggnaden, August 2023. publisher: Dagens industri.

[2] Energimarknadsinspektionen. Föreskrift EIFS 2013:1, August 2013.

[3] Afshin Samadi. *Large scale solar power integration in distribution grids: PV modelling, voltage support and aggregation studies*. Number 2014:050 in TRITA-EE,. Electrical Engineering, Stockholm, 2014. OCLC: 941094901.

[4] Thomas Stetz, Frank Marten, and Martin Braun. Improved Low Voltage Grid-Integration of Photovoltaic Systems in Germany. *IEEE Transactions on Sustainable Energy*, 4(2):534–542, April 2013.

[5] Seyedmostafa Hashemi, Jacob Østergaard, Thomas Degner, Ron Brandl, and Wolfram Heckmann. Efficient control of active transformers for increasing the pv hosting capacity of lv grids. *IEEE Transactions on Industrial Informatics*, 13(1):270–277, 2017.

[6] Ingmar Leisse. *Efficient integration of distributed generation in electricity distribution networks: voltage control and network design*. Department of Measurement Technology and Industrial Electrical Engineering, Lund, 2013. OCLC: 940610420.

[7] Martin Lundberg, Olof Samuelsson, and Emil Hillberg. Local voltage control in distribution networks using PI control of active and reactive power. *Electric Power Systems Research*, 212:108475, November 2022.

[8] Svenska Kraftnät. Sveriges elnät, December 2022.

[9] William H. Kersting. *Distribution system modeling and analysis, Third Edition*. CRC Press, Abingdon, 3rd ed., revised. edition, January 2012. OCLC: 895705799.

[10] Musharraf Wajahat, Hassan Abdullah Khalid, Ghullam Mustafa Bhutto, and Claus Leth Bak. A comparative study into enhancing the pv penetration limit of a lv cigre residential network with distributed grid-tied single-phase pv systems. *Energies*, 2019.

[11] J.A. Peças Lopes, N. Hatziargyriou, J. Mutale, P. Djapic, and N. Jenkins. Integrating distributed generation into electric power systems: A review of drivers, challenges and opportunities. *Electric Power Systems Research*, 77(9):1189–1203, 2007. Distributed Generation.

[12] Emil Hillberg, Hjalmar Pihl, Stina Hallhagen, Olof Samuelsson, Martin Lundberg, Markus Mirz, Bettina Schäfer, Johannes Weber, Tereza Borges, Lars-Gunnar Fagerberg, Martin Jältås, Maria Edvall, Máté Csőre, Ádám Tóth, István Táczi, Gábor Mihály Péter, Jörgen Rosvall, Neil Hancock, Inigo Berazaluce, and Sanjana Tambavekar. Active Network Management for All – ANM4L a collaborative research project. 2020.

[13] Conseil international des grands réseaux électriques, editor. *Benchmark systems for network integration of renewable and distributed energy resources*. CIGRÉ, Paris, 2014.

[14] Muammar Zainuddin, Frengki Eka Putra Surusa, Syafaruddin, and Salama Manjang. Constant Power Factor Mode of Grid-Connected Photovoltaic Inverter for Harmonics Distortion Assessment. *International Journal of Renewable Energy Research*, (v10i3), 2020.

[15] Torkel Glad and Lennart Ljung. *Reglerteknik Grundläggande teori*. Studentlitteratur, 2006.

[16] Conseil international des grands réseaux électriques, editor. *Distributed energy resource benchmark models for quasi-static time-series power flow simulations*. Number 906 in Technical brochure / CIGRE. CIGRE, Paris, France, 2023.